Mechanics of Notched Izod Impact Testing of Polycarbonate

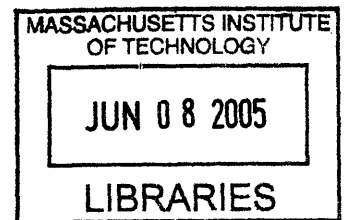by

Meredith N. Silberstein

SUBMITTED TO THE DEPARTMENT OF MECHANICAL ENGINEERING IN PARTIAL
FULFILLMENT OF THE REQUIREMENTS FOR THE DEGREE OF
BACHELOR OF SCIENCE IN MECHANICAL ENGINEERING

AT THE

MASSACHUSETTS INSTITUTE OF TECHNOLOGY

JUNE 2005

Signature of Author:_____
Department of Mechanical Engineering
May 23, 2005

Certified by:_____
Mary C. Boyce
Kendall Family Professor of Mechanical Engineering
Thesis Supervisor

Accepted by:_____
Ernest G. Cravalho
Professor of Mechanical Engineering
Chairman of the Undergraduate Thesis Committee

Mechanics of Notched Izod Impact Testing of Polycarbonate

by

Meredith N. Silberstein

SUBMITTED TO THE DEPARTMENT OF MECHANICAL ENGINEERING IN PARTIAL FULFILLMENT OF THE REQUIREMENTS FOR THE DEGREE OF

BACHELOR OF SCIENCE IN MECHANICAL ENGINEERING
AT THE
MASSACHUSETTS INSTITUTE OF TECHNOLOGY

ABSTRACT

Polycarbonate is widely used as a transparent protective material because of its low density and excellent mechanical properties. However, when defects such as cracks or notches are introduced, it is subject to catastrophic brittle failure at relatively low loads. Notched Izod testing is a common qualitative measure of toughness of a material, measuring energy absorbed prior to failure under high triaxiality and high rate loading conditions. Much research has been done using Izod testing to compare the fracture energies of blends of Polycarbonate and rubbery materials; however the specific yielding and fracture mechanisms associated with each blend are rarely analyzed. This study presents detailed images, fracture energies, and time durations of the deformation and failure processes actively occurring during the Notched Izod testing of 3.23mm and 6.35mm thick Polycarbonate specimens, as well as of a quasi-static version of Notched Izod bending. The thin specimens were found to yield in a ductile manner followed by tearing across most of the ligament width, resulting in a final failure including a small plastically-deformed ligament hinging the two failure surfaces in both the Notched Izod impact and Quasi-Static tests. The thick specimens exhibited slight yielding followed by catastrophic failure, where the crack initiated ahead of the notch and then propagating back towards the notch root as well as across the remaining ligament.. In the thick Izod tests local pre-failure yielding was evident at the notch root resulting in extensive blunting of the notch. The fracture energies per unit thickness for the thin specimens were almost a full order of magnitude larger than those for the thick specimens. A finite element simulation for the Notched Izod Impact test was developed using the Arruda and Boyce(1988) constitutive model of polymers as modified by Mulliken and Boyce(2004) for high rate deformation. The 3.23mm Notched Izod impact test was successfully modeled from initial contact of the pendulum through initiation of failure and early tearing. The yielding patterns and failure occurred along the same lines as in the experiment where diagonal shear bands and lobes initiate plastic deformation from the notch tip and tearing progresses in a horizontal manner across the specimen width. An extensive shear yielded region is observed ahead of the propagating tear. The 6.35mm thick model shows the beginning of the formation pressure concentration which causes brittle fracture, but further refinement of the mesh needs to be performed for more accurate modeling.

Thesis Supervisor: Mary C. Boyce

Title: Kendall Family Professor of Mechanical Engineering

Table of Contents

List of Figures

List of Tables

Chapter One: Introduction

Polycarbonate is widely used today due to its low density and excellent mechanical properties combined with its transparency. Popular applications include helmets, body armor, lenses, windows, and safety goggles. Polycarbonate is relatively tough compared to many other polymers, while it is able to undergo large deformation during low triaxiality tensile and bending loading conditions. However, under conditions of high triaxiality such as at sharp notches and cracks, and also under high rate loading conditions, PC can exhibit brittle failure. Therefore, a specimen or component may fail catastrophically at a much lower force than expected. Understanding this effect as a function of impact rate, notch geometry, and sample thickness can provide insight into how polycarbonate should and should not be used. Notched Izod impact testing is an experimental method to quantify the energy absorbed by the polymer during the adverse loading conditions of high triaxiality and high rate. Extensive Izod testing of polycarbonate has been performed, especially for use in comparison with polycarbonate blends with rubbery particles, but little modeling has been done to understand and predict the behavior of polycarbonate during Izod testing in an absolute manner. The recent addition of high strain rate characteristics [Mulliken and Boyce, 2004] to the Boyce et al. (1988) constitutive model of polymers makes this modeling realistic.

When a polymer is loaded in tension, it can either yield and then plastically deform in a ductile manner or it can fracture in a brittle manner. A brittle failure is when the specimen deforms in a linear elastic manner to a peak load and breaks at this maximum load, typically at strains less than 10%; little energy is absorbed by the polymer during such brittle failures. Ductile behavior is when the specimen will exhibit elastic behavior, followed by yield and extensive post-yield plastic deformation to rather large strains; extensive energy is absorbed by the plastic deformation. The ductile failure mode consumes significantly more energy than brittle failure. The mode of failure at any given strain rate and temperature depends on the value of the yield or flow stress relative to the brittle or fracture stress. The material will fail in whichever mode has a lower value. The brittle fracture stress is fairly constant over strain and temperature, decreasing only slightly with increasing temperature and increasing only slightly with increasing strain rate. A variety of testing methods are used to evaluate the toughness of a material, three of the most common are uniaxial tension, fracture toughness, and the Izod impact test.
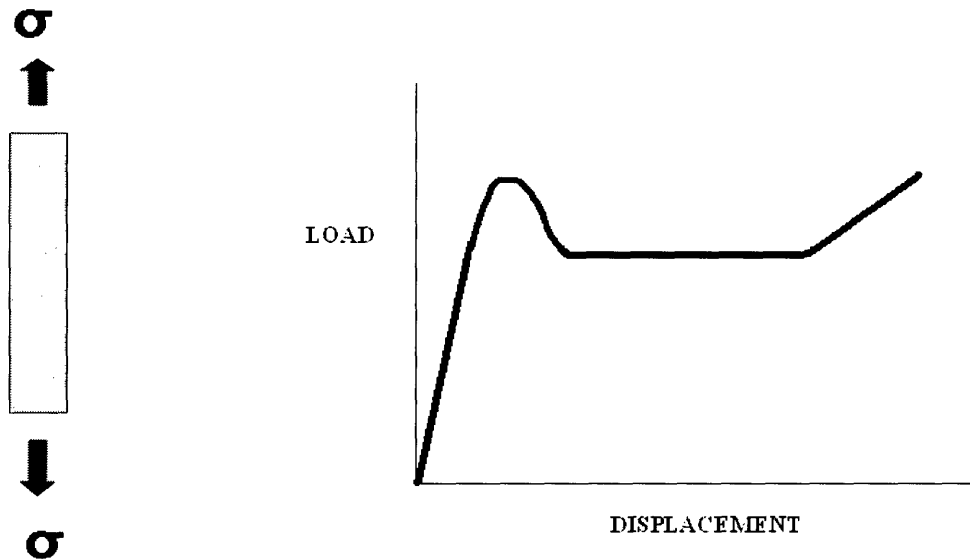
Figure 1.1 Loading in uniaxial tension test for toughness and typical load extension curve for polycarbonate.

In a uniaxial tension test a bar of material is loaded in tension along one axis (shown in Figure 1.1) and its load versus displacement behavior is monitored until failure; the area under the load-displacement curve divided by the volume of material deformed is one measure of toughness of the material – the tensile toughness. This is a low triaxial loading condition, where triaxiality is defined as the ratio of the hydrostatic stress, σ_H, to the Mises equivalent stress, σ_M:

$$\sigma_H = \frac{1}{3}(\sigma_1 + \sigma_2 + \sigma_3)$$ [1.1]

$$\sigma_M = \sqrt{0.5\left((\sigma_1 - \sigma_2)^2 + (\sigma_2 - \sigma_3)^2 + (\sigma_3 - \sigma_1)^2\right)}$$ [1.2]

$$\Sigma = \frac{\sigma_H}{\sigma_M}$$ [1.3]

For uniaxial tension the triaxiality is equal to 1/3. Low triaxiality conditions typically favor yielding over brittle fracture since a high hydrostatic stress would be needed to break apart the specimen catastrophically. However, there are several polymers which fail in a brittle manner even during uniaxial tension (for example, polymethylmethacrylate (Plexiglass) and polystyrene); polycarbonate is ductile during uniaxial tension.

Fracture mechanics can be used to understand the stress required for brittle fracture given an idealized sharp crack of length 2c. The stress field around the crack is identical for all types of loading, but its magnitude is determined by the stress intensity factor K_I which is a function of given loads and geometries. For an infinite sheet with a central crack

$$K_I = \sigma(\pi c)^{1/2} \qquad\qquad [1.4]$$

where σ is the far field tensile stress in the direction normal to the crack plane. The loading method is depicted in Figure 1.2 below.
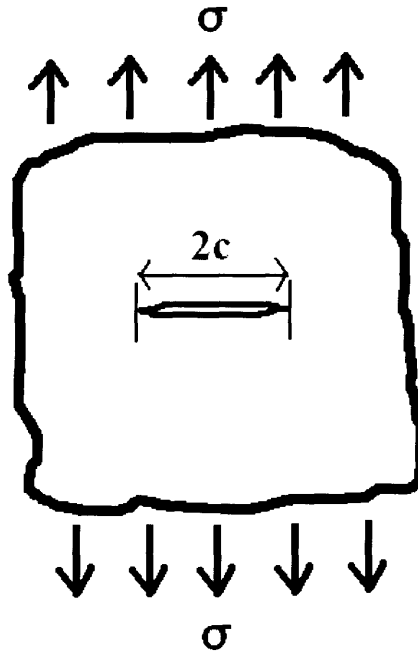

Figure 1.2 Fracture mechanics loading condition.

The stress intensity factor has a critical value called the fracture toughness K_c. K_c depends on the thickness of the specimen.
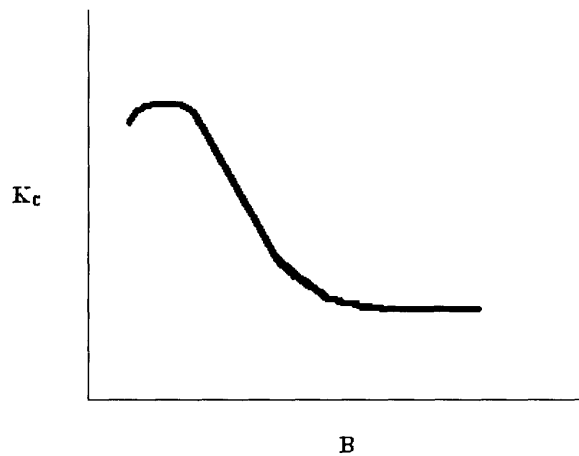

Figure 1.3 Critical fracture toughness K_c versus thickness

The brittle fracture stress can then be predicted from a known critical stress intensity factor.

$$\sigma_B = \frac{K_{Ic}}{Q\sqrt{\pi a}}$$ [1.5]

where Q is the geometry factor that accounts for the change in the geometry dependence of the stress intensity factor relative to the stress intensity factor for an infinite plate with a central crack. Fracture toughness is one measure of toughness that has found extensive use in quantitatively predicting fracture initiation for different geometries and loading conditions, where Q has been analytically and/or numerically determined for many geometries and loading

The Notched Izod impact test is a third technique to obtain a measure of toughness. It measures the energy required to fracture a notched specimen at relatively high rate bending conditions. The apparatus for the Izod impact test is shown in Figure 1.4 below. A pendulum with adjustable weight is released from a known height; a rounded point on the tip of the pendulum makes contact with a notched specimen 22mm above the center of the notch. The specimen is positioned so that the notch is on the side facing the pendulum.

The combination of a notched condition and high rates provides dramatically adverse loading conditions for evaluating a material's energy to failure. The sharpness of the notch together with the thickness of the specimen combines to provide high triaxiality ahead of the notch.

For thick specimens plane strain can be assumed. When the notched specimen is impacted, the stress and strain will be concentrated in the region of the notch tip. The area around the notch will begin to deform plastically. The yielding zone will be much smaller than the thickness of the specimen. As the notch tip area stretches vertically from the impact, it will try to contract laterally through the thickness due to the plastic incompressibility of polycarbonate. The outer sections of the specimen however will be in the elastic regime and will resist the lateral contraction of the plastically deforming region, creating a plane strain constraint condition locally at the notch root which creates an additional tensile normal stress in the through-thickness direction, creating locally very high triaxiality loading conditions. Crazing or some form of cavitation will often then be favored over yielding due to the locally high hydrostatic stress. The crazing causes a separation of the surfaces above and below the crack tip. A thin surface layer of the polycarbonate does not experience the additional through thickness normal stress since it is traction free and this thin layer will undergo shear yielding.. This results in a fracture surface profile that is flat across the middle and has a small shear lip on each end.
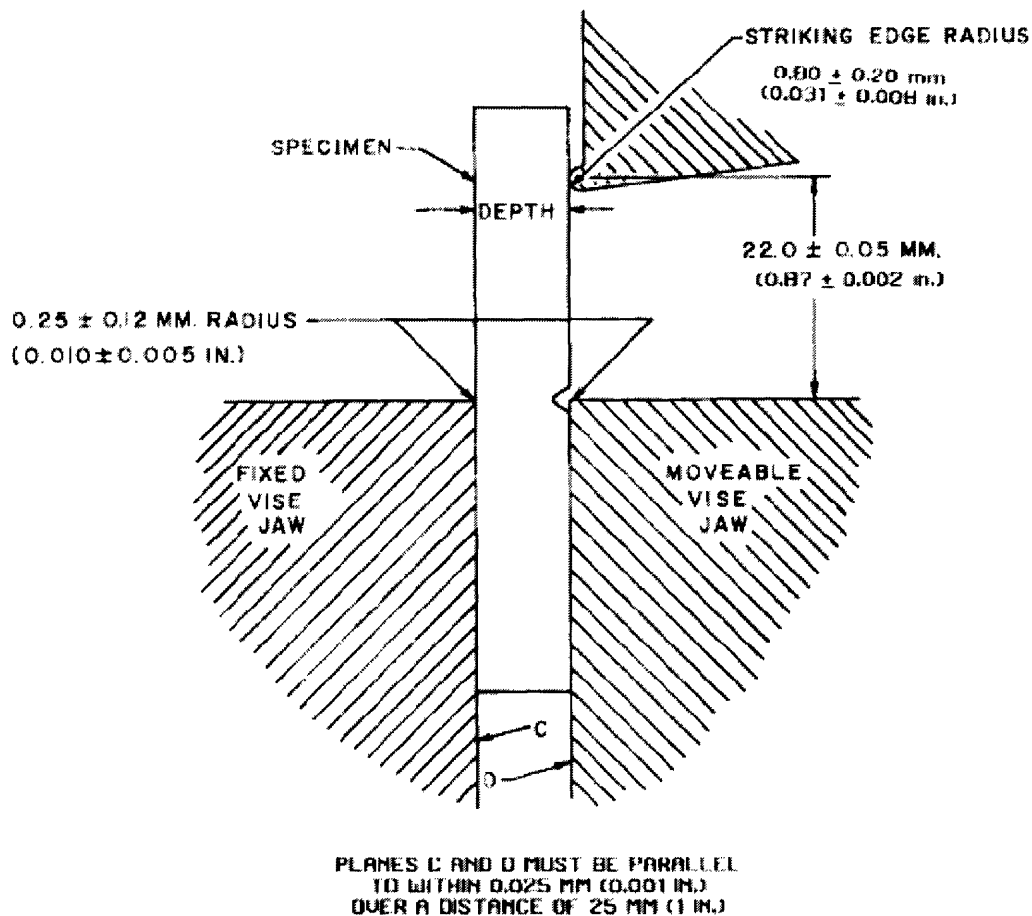
Figure 1.4 Notched Izod impact test apparatus [Standard Test Methods for Determining the Izod Pendulum Impact Resistance of Plastics].

For thin specimens plane stress can be assumed. The specimen is thin enough such that the surrounding elastically deformed material does not constrain the thinning of the local plastically deforming region. This enables a local necking through the thickness. Rather than failing catastrophically, the notch region will deform plastically until the excessive strain levels are reached and a tearing failure occurs beginning at the notch. The tear will gradually propagate as the fracture condition is reached at the leading point of the tear until the specimen has fractured completely. This method of fracture consumes significantly more energy than the instantaneous fracture of the thicker specimens.

The behavior of a material in notched Izod style bending is dependent on both the temperature and strain rate. Brittle fracture versus yield and plastic tearing is determined by whether the yield stress or the critical conditions for crack initiation is reached first. While the critical crack initiation conditions are relatively independent of temperature and strain rate, yield stress is highly dependent on both factors. The yield stress decreases by a factor of ten over a temperature range from -180°C to 20°C. Therefore the exact same notch with the same impact, might undergo brittle fracture at one temperature and yield at another temperature. The inverse effect occurs with strain rate; as strain rate increases the yield stress decreases.
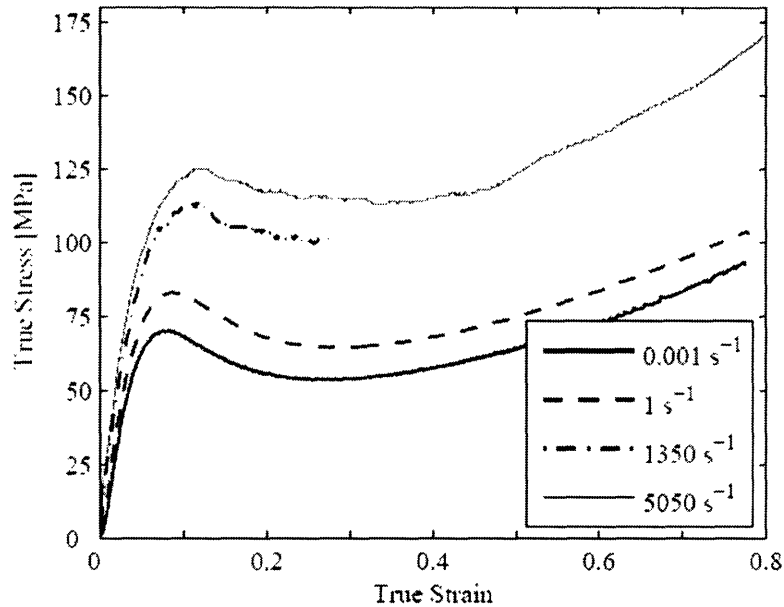
Figure 1.5 Variation of stress-strain curve with changes in strain rate [Mulliken and Boyce, 2005].

Much research has been conducted concerning high impact sensitivity of Polycarbonate and Polycarbonate blends with rubbery materials. The Izod impact test is used to compare the fracture toughness of different blends at a variety of temperatures. Cheng et al. (1994) tested standard Izod specimens of two thicknesses: 3.18mm and 6.35mm. He found that the transition from brittle to ductile failure occurred between those two thicknesses. At 25°C the wider specimens averaged an impact fracture energy of 112 J/m while the thinner specimens averaged an impact fracture energy of 918 J/m. Lombardo et al.(1994) studied sharp and standard notch samples 3.18mm thick. The sharp notches were created by pressing a new razor blade into the standard machined notch. The sharp notches had a fracture energy of 80 J/m. The standard notch impact fracture energy was found to be 1000 J/m at room temperature. The notch transition temperature was -25°C. There was a ±5% variability in the data overall, but it was greater in the transition region for the standard notches. Stetz et al. (1999) did sharp and standard notch testing at temperatures from -40°C to 30 °C. The sharp notches were all found to be brittle at all temperatures with impact fracture energy around 75 J/m. The standard notched samples were brittle at lower temperatures and ductile at higher temperatures with a notch transition temperature of -20 °C. At -40°C the impact fracture energy was found to be 75 J/m, at 30°C the impact fracture energy was found to be 900 J/m.

In this thesis research Notched Izod impact testing was performed on ASTM standard specimens of thickness 3.23mm and 6.35mm. A Quasi-Static version of the same Notched Izod bending mode was designed and performed as well, with a loading rod replacing the pendulum and moving at a constant velocity of 2mm per min. Both sets of experiments were recorded with appropriately capable cameras so that the yielding and fracture progression could be analyzed in detail. A detailed procedure of how both tests

11

were conducted will be followed by a presentation of the results for each. A finite element model is then presented that simulates the failure modes of each thickness for both the Notched Izod Impact and Quasi-Static Izod tests.

Chapter Two: Experiments

2.1 Material

All the experiments were conducted with the commercial high impact Polycarbonate Lexan9034 from General Electric. The Izod fracture energy is listed as from 641 to 853 J/m for 1/8" thick samples. [LEXAN® 9034 Product Data Sheet, GE Structured Products] The specimens were cut according to ASTM Izod standards. The specimen dimensions are depicted in Figure 2.1 below. Detailed manufacturing instructions are in the ASTM standard.
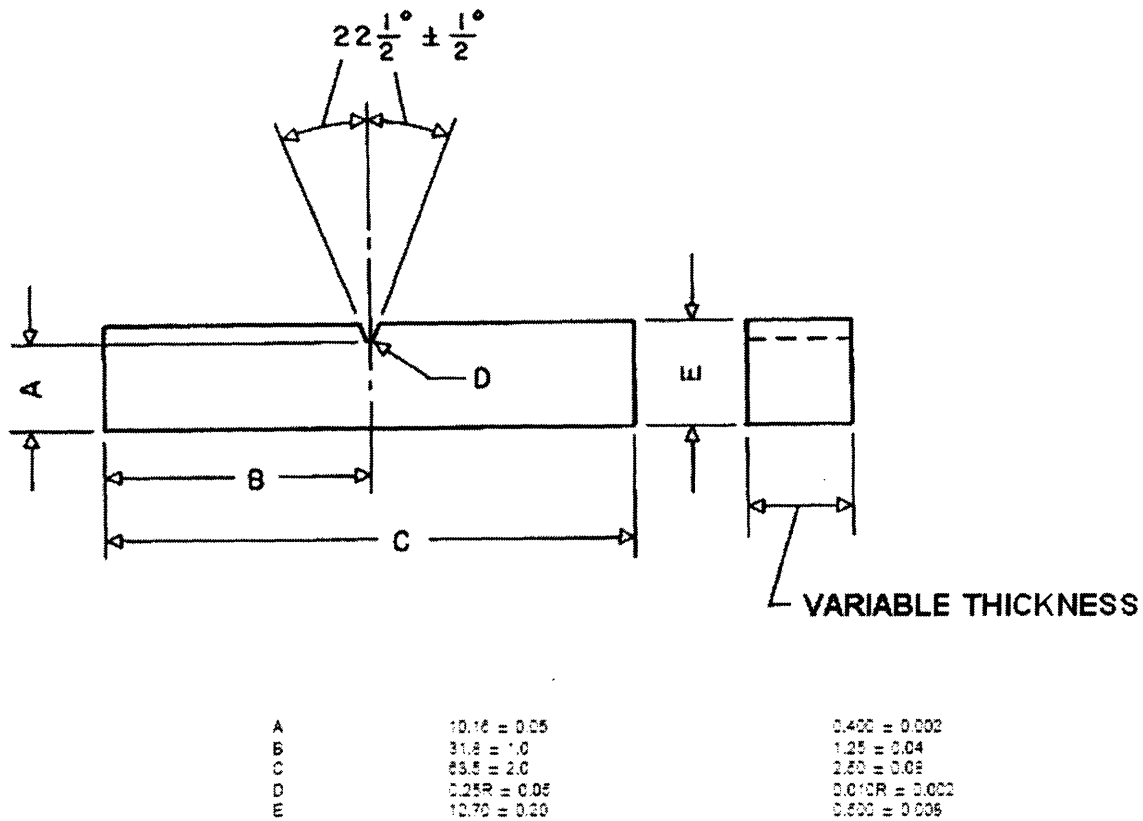

A	10.16 ± 0.05	0.400 ± 0.002
B	31.8 ± 1.0	1.25 ± 0.04
C	63.5 ± 2.0	2.50 ± 0.09
D	0.25R ± 0.05	0.010R ± 0.002
E	12.70 ± 0.20	0.500 ± 0.008

Figure 2.1 Standard Izod specimen dimensions. All dimensions are given in mm. [Standard Test Methods for Determining the Izod Pendulum Impact Resistance of Plastics].

There is no ASTM standard thickness for Izod testing; it only has to be between 3.0mm and 12.7mm. The most common commercial thickness used is 3.2mm. For these experiments thicknesses of 3.23mm and 6.35mm were used.

Since the notch radius is critical to the impact fracture energy, the radius for each specimen was measured. An optical microscope was focused on the top surface of the Izod specimen at a magnification of approximately 60x. A digital picture was then taken of the notch. A Filar scale printed on a sheet of paper was then placed on top of the

specimen and a digital picture was taken. The same scale was used for all specimens of the same thickness. The image of the scale was used to draw concentric circles at known demagnified radii. The image of the notch was then lined up with the concentric circle that matched in order to determine its radius. The notch angle was also measured from each image. The filar scale image for the 6.35mm wide specimens and the notch from one of the 6.35mm specimens are shown in Figure 2.2 below.
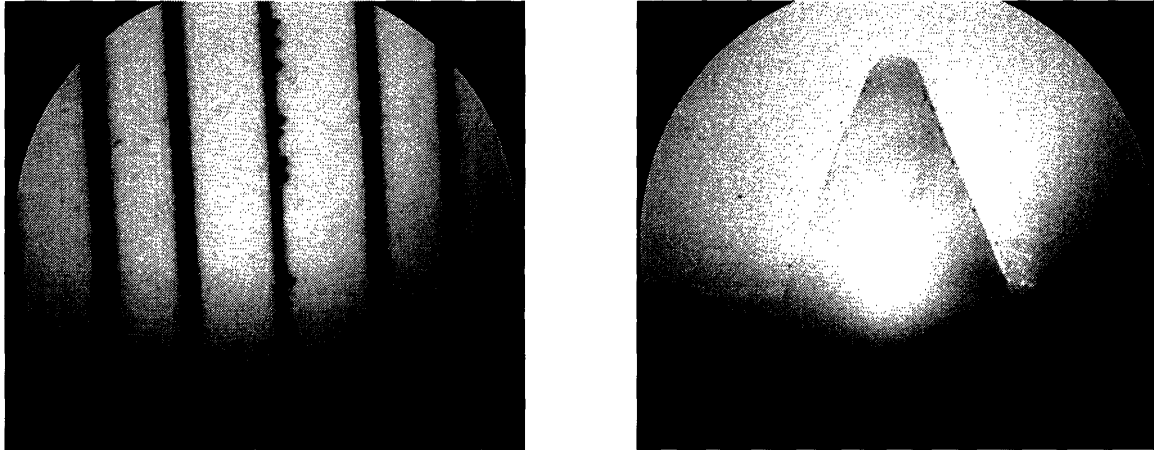

Figure 2.2 Filar scale image for the 6.35mm wide specimens and the notch from one of the 6.35mm specimens.

The notch radii and angles are displayed is Table 2.1 below. The angle of more than half of the notches are within the 45±1° range given by the ASTM standard. The remaining notches are within another 1.5°. The same accuracy is not there for the radii of the notches. The radii are approximately one- third of the expected value. This means that instead of working with standard notches, the tests are being conducted on sharp notches. This will tend to lead to a more brittle fracture at lower strain rates and higher temperatures, and lower breaking energies overall.

Table 2.1 Notch Dimensions

	Width(mm)	Radius(μm)	Angle(°)
N1	6.35	7.5	45
N2	6.35	7.5	46
N3	6.35	8	45
N4	6.35	7	46
N5	6.35	7	47
N6	6.35	8	45
N7	6.35	9	45
N8	6.35	7.5	45
N9	6.35	6	46
N10	6.35	7.5	44
N11	6.35	7	47
N12	3.23	8	47
N13	3.23	9	46
N14	3.23	8	47
N15	3.23	5	46.5
N16	3.23	6	45
N17	3.23	6	44.5
N18	3.23	8	47
N19	3.23	8	43.5
N20	3.23	9	46
N21	3.23	9	47.5

2.2 Experimental Procedure

2.2.1 Notched Izod Impact Experimental Procedure

A Tinius Olsen T-92 Izod impact tester was used to test the impact fracture energy of polycarbonate. Before each testing session the machine was calibrated according to the instruction manual by letting it free hang to determine the zero-position and by releasing the pendulum with no specimen in place to determine the energy losses due to windage and friction. The windage and friction loss calculation was done automatically by the T-92. A type "C" test was performed on all samples. The specimen was placed with the notch oriented towards the leading edge of the pendulum. The vertical position was determined by an alignment fixture which mated with the top half of the notch and was positioned to guarantee that the pendulum hit at the appropriate specimen height relative to the notch each time. The specimen was then clamped with pressure on the surfaces normal to the direction of the pendulum swing. The T-92 was set to test mode. The sample width was entered and then the pendulum was released according to screen instructions. The pendulum was then reset. The top half of the specimen was placed back on top of the bottom half which was still clamped in. The pendulum was released again so that a toss correction could be performed. The toss correction subtracts out the energy from the initial swing that went into throwing the sample, leaving only the breaking energy.

For the 6.35mm samples, images were taken of the Notched Izod impact test using a Cordin model 550 high speed rotating mirror CCD framing camera. The high speed camera uses multiple camera modules to achieve frame rates up to 800,000 frames per second. The slower the speed, the higher the exposure time for each image. It is limited to a total of 32 frames. It has a resolution of 1000×1000 pixels. A 5-volt trigger signal from the T-92 was used to trigger the high speed camera. It was set to trigger at $3.0\mu m$ from the point at which the pendulum hits the sample. An additional delay feature in the high speed camera was used to fine tune the trigger point. A flash was triggered by the same signal with a delay $240\mu s$ smaller than that for the camera so that the sample would be illuminated while the pictures were taken. The initial yielding, crack initiation and propagation, and initial motion after separation were captured.

For the 3.23mm samples and two of the 6.35mm samples, video was taken using the medium speed Phantom Camera. The Phantom can reach rates between 1,000 and 95,000 frames per second. Its simpler one camera module configuration allows it to record for a longer period of time. This was useful for the thinner samples which fracture at a slower rate than 6.35mm samples. The Phantom recorded the event in detail. The speed the Phantom Camera is able to reach decreases with increasing resolution. A speed of 11,363 frames per second was used with a resolution of 256 ×256 pixels. A small halogen light was used to illuminate the specimen from the front, with a white plane behind it to reflect light back through the translucent specimen. Due to the heat intensity of the light and the small heat capacity of the specimen it was only turned on for focusing purposes and immediately before the pendulum was released. The specimen was allowed to cool down to room temperature after focusing before the test was performed.

2.2.2 Quasi-Static Izod Experimental Procedure

A test fixture was developed to simulate the bending geometry of the Notched Izod impact tested quasi-statically. A Zwick/Roelle Z010 with a load cell maximum of 10kN was used in compression mode. The bottom grip was custom designed to allow clamping in the same locations as the Notched Izod, for the indenter to load the specimen in the same location as the pendulum, and for the specimen to be able to deform the full 90°. The test fixture is depicted in Figure 2.3 below. Detailed diagrams are included in Appendix A.
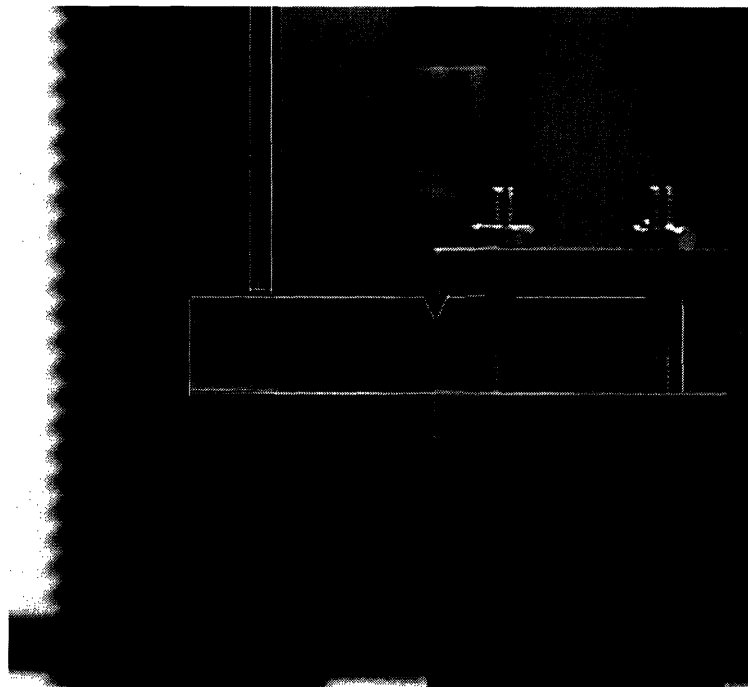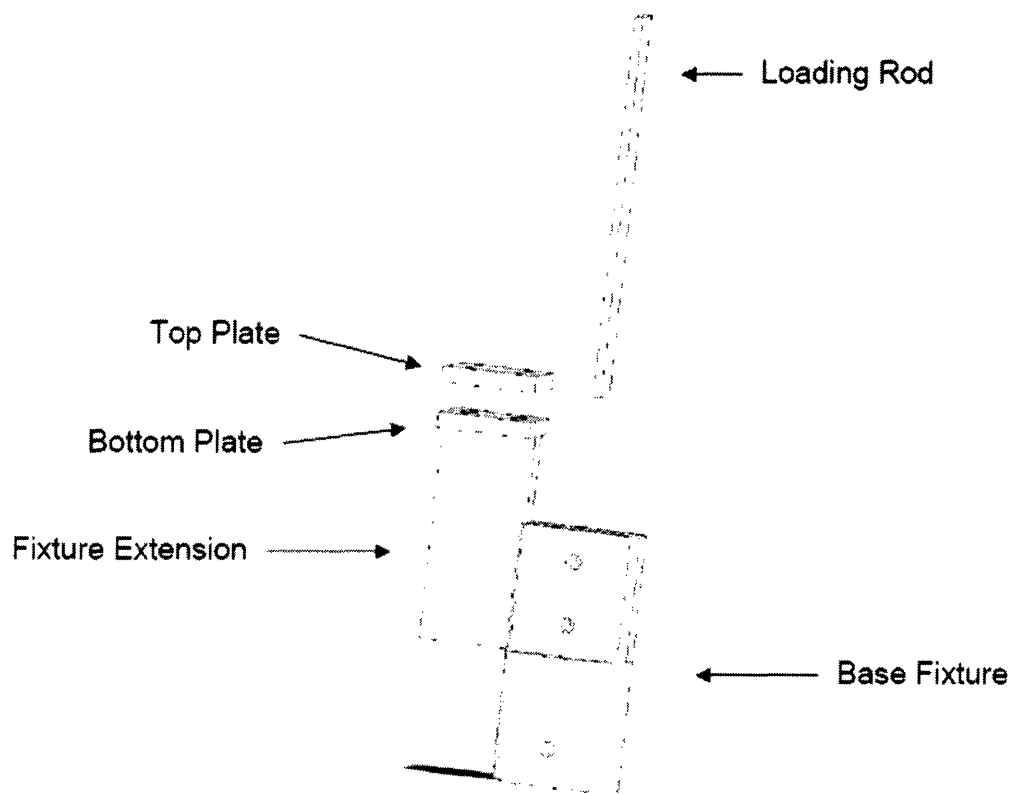
Loading Rod

Top Plate

Bottom Plate

Fixture Extension

Base Fixture

Figure 2.3 Custom fixture used to apply Izod type bending Quasi-Statically.

The specimen was placed in between the rectangular plates along the centerline with the notch facing up and centered on the edge of the bottom plate. The top plate was then bolted down to the bottom plate. A tension grip was used on top to hold the indenter.

The computer program *TestExpert* was used to interface with the Zwick. The force on the compression fixtures was zeroed and the grips were moved so that the indenter was 5mm above the face of the IZOD specimen. The program was configured to move the indenter down at 2mm per minute until it reached a preload of 2N. The force and position data collection system was then started along with a video camera centered on the notch area. For the 6.35mm specimens the indenter moved down at 2mm per minute until the specimens broke. For the 3.23mm thick specimens the indenter moved down at 2mm per minute for 10 to 35mm depending on the particular test run. The indenter was then rapidly lifted to its initial position on 5mm above the specimen. The camera continued recording for several seconds following the removal of the force so that the elastic recovery could be recorded as well.

The camera used was a commercial analog video camera which was connected to the computer via a video output cable. A frame was taken from the analog feed and digitized once a second. The camera was placed approximately two feet from the specimen and its zoom feature was used to focus on the specimen. For higher magnification tests the camera was positioned one foot away from the surface of the specimen and a magnifying glass was placed immediately in front of the camera lens.

2.3 Results and Discussion

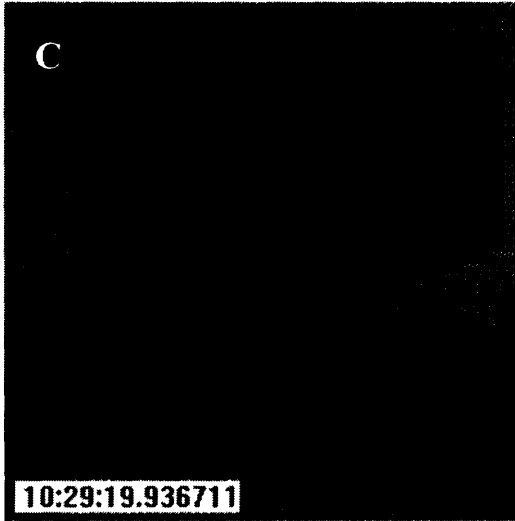### 2.3.1 Notched Izod Impact Test Results and Discussion

Table 2.2 shows the breaking energy and fracture energy for each of the specimens tested. The fracture energy is calculated by dividing the experimentally determined breaking energy by the thickness of the specimen. The maximum pendulum energy is determined by the weights attached to the pendulum. The ASTM Izod standard recommends that less than 85% of the pendulums total energy is used to break the specimen.

Table 2.2 Notched Izod impact breaking energies and fracture energy per thickness for all samples tested.

Specimen	Pendulum Max Energy(J)	Breaking Energy(J)	Fracture Energy per Thickness (J/m)
thickness=6.35mm			
N3	2.82	0.7873	123.98
N4	2.82	0.7399	116.52
N5	2.82	0.7942	125.07
N6	2.82	0.7257	114.29
N10	11.3	0.7564	119.13
N11	11.3	0.7474	117.2
thickness=3.23mm			
N18	11.3	2.5764	853.37
N16	22.6	2.8849	893.05
N17	22.6	2.8069	860.29

Images extracted from a video taken of the Izod test of specimen N11 are shown in Figure 2.4 below. Notice how this sample whose thickness places it at the borderline of totally brittle, has a small amount of yielding followed by high speed crack formation.

A

10:29:19.936533

B

10:29:19.936622

C
10:29:19.936711

D
10:29:19.936801

E
10:29:19.936889

F
10:29:19.937067

G
10:29:19.937067

H
10:29:19.937157

20
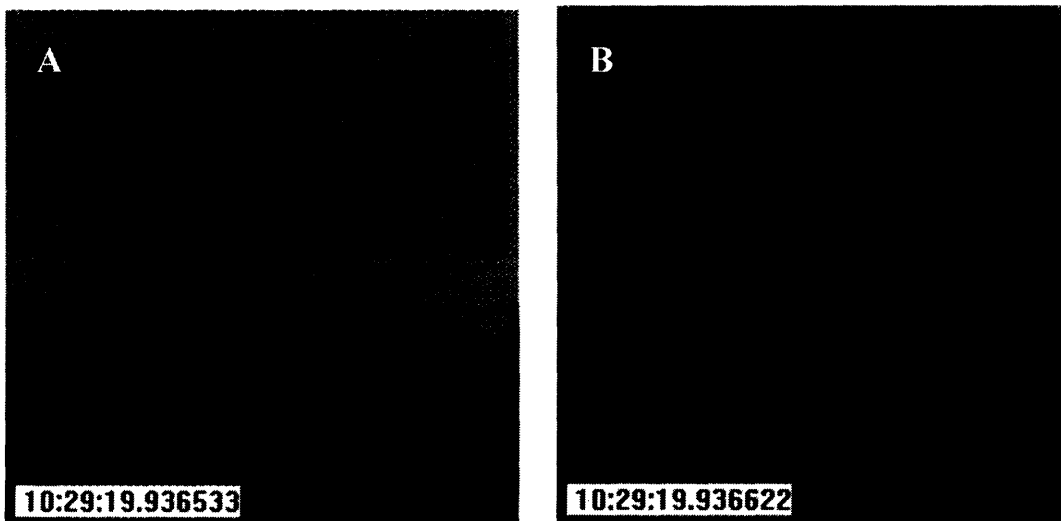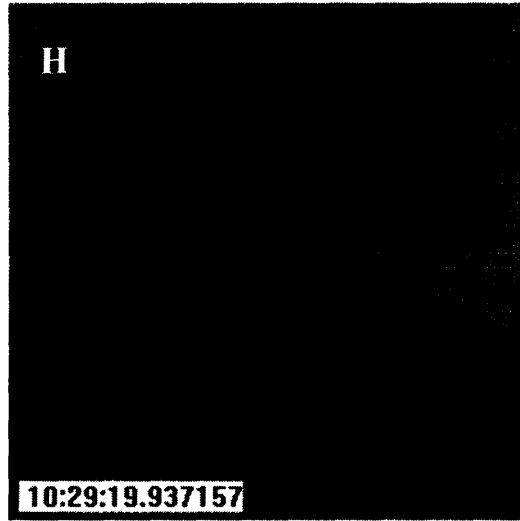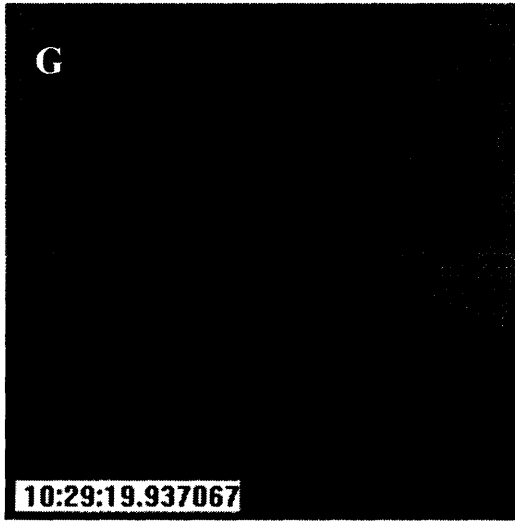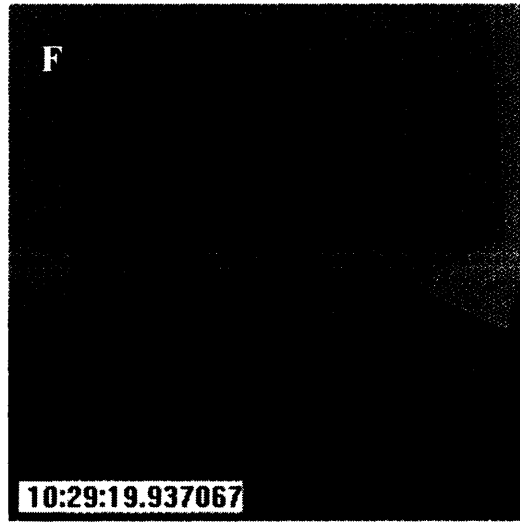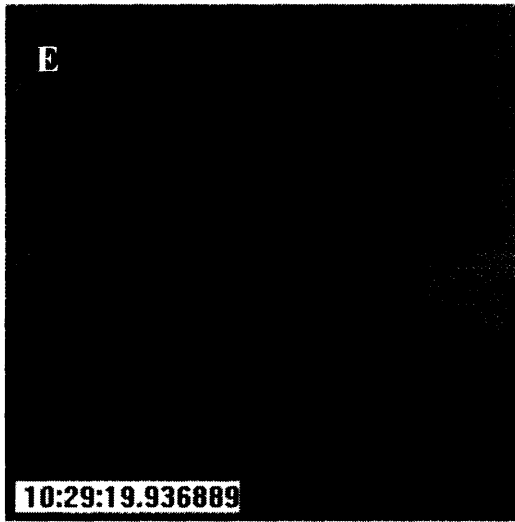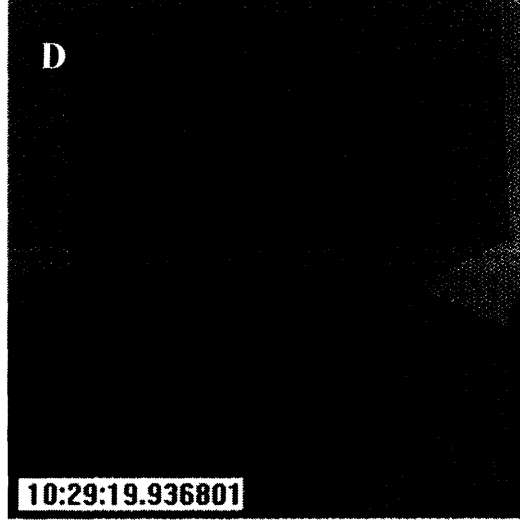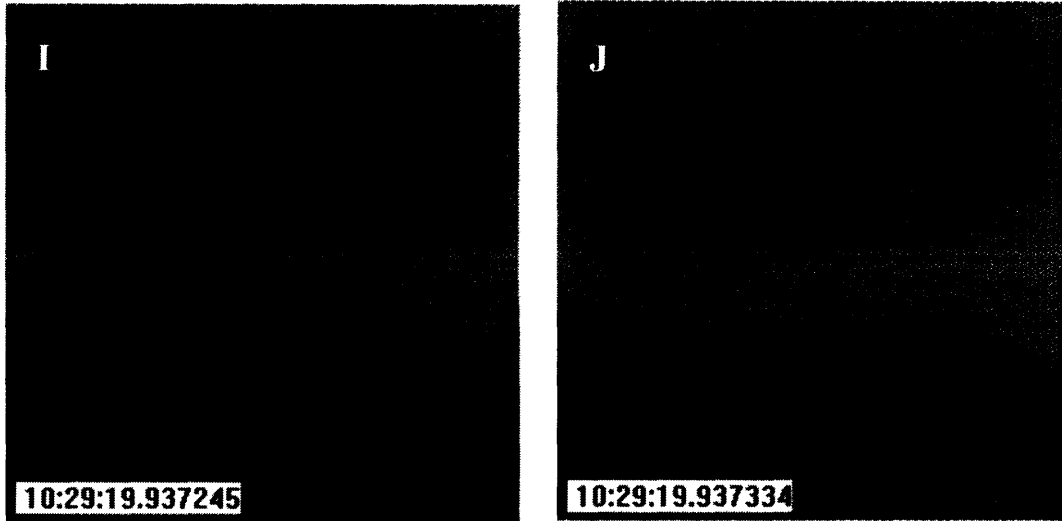
Figure 2.4 Phantom camera images of Notched Izod Impact test of 6.35mm thick specimen.

In the higher speed images of sample N6, also of width 6.35mm, the crack propagation is more clearly seen. In the first image of Figure 2.5 a small amount of yielding has occurred but the crack has not begun to form. In the second image a thin crack has formed not at the notch tip, but ahead of the notch tip. In the third image the crack has propagated three quarters of the way back. The time difference between each image is 26.6μs.
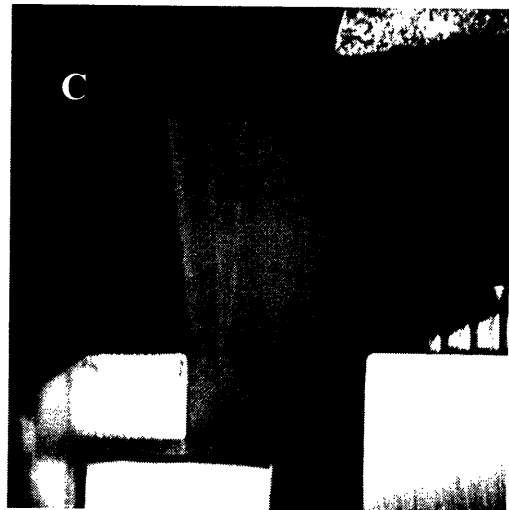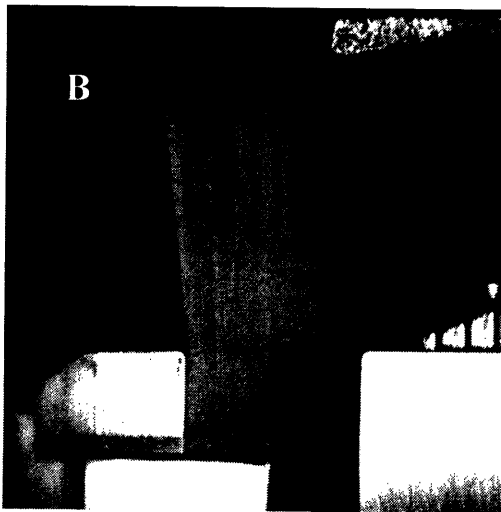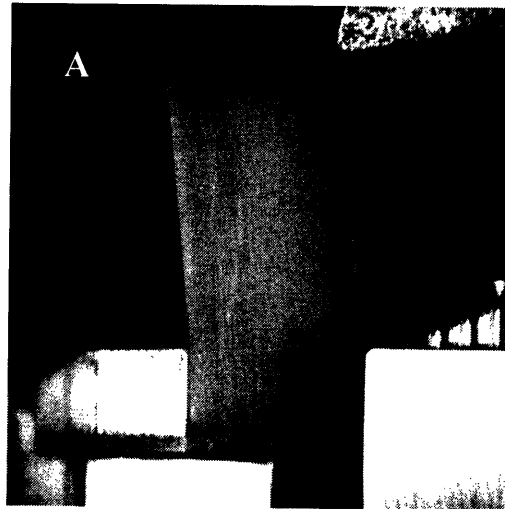
(a)
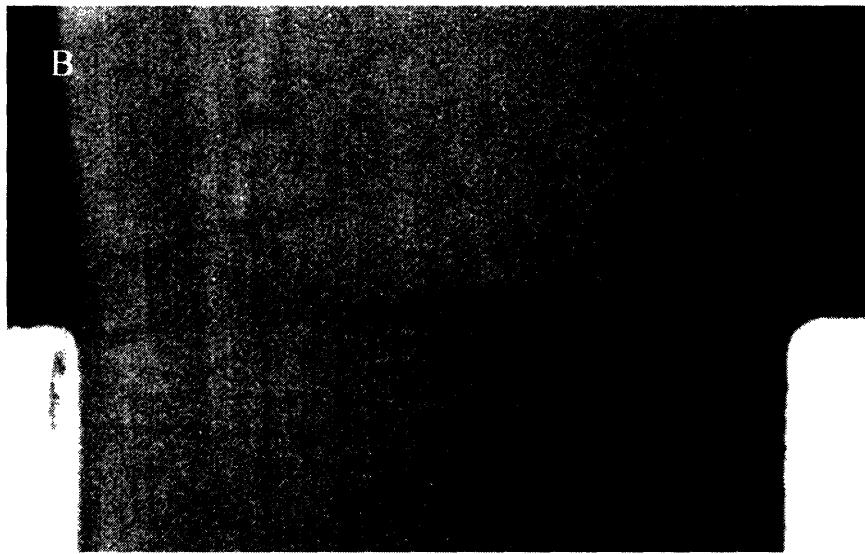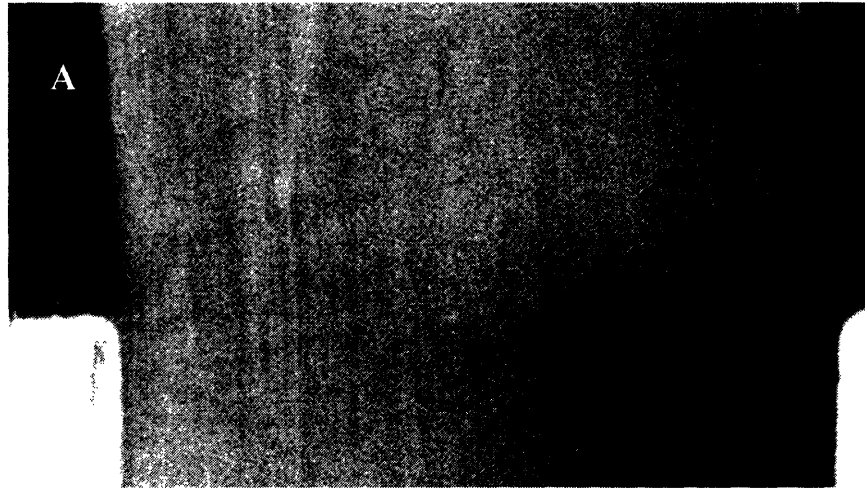
(b)

Figure 2.5 Crack formation in Notched Izod impact test of sample of 6.35mm. **(a)** wide
view including pendulum **(b)** enlarged view of notch region

The speed of crack propagation can be calculated from the second and third images. The crack extends 1.894mm in one frame, so the crack propagation speed is 71.2m/s.

The thinner samples did not break completely, but did tear through approximately 90% in the direction of pendulum motion. In the first thin sample test, the pendulum slowed down significantly, so the weight was increased for the remaining tests. When the weight was nearly doubled, the breaking energy increased noticeably, but remained significantly below the capacity of the pendulum. The specimen tore slightly further but still did not rip completely. Figure 2.6 shows the yielding and tearing process for a test done with the pendulum configured with a maximum energy of 22.6J.

C 12:25:04.775249

D 12:25:04.776138

E 12:25:04.776583

F 12:25:04.777029

G 12:25:04.777473

H 12:25:04.786551
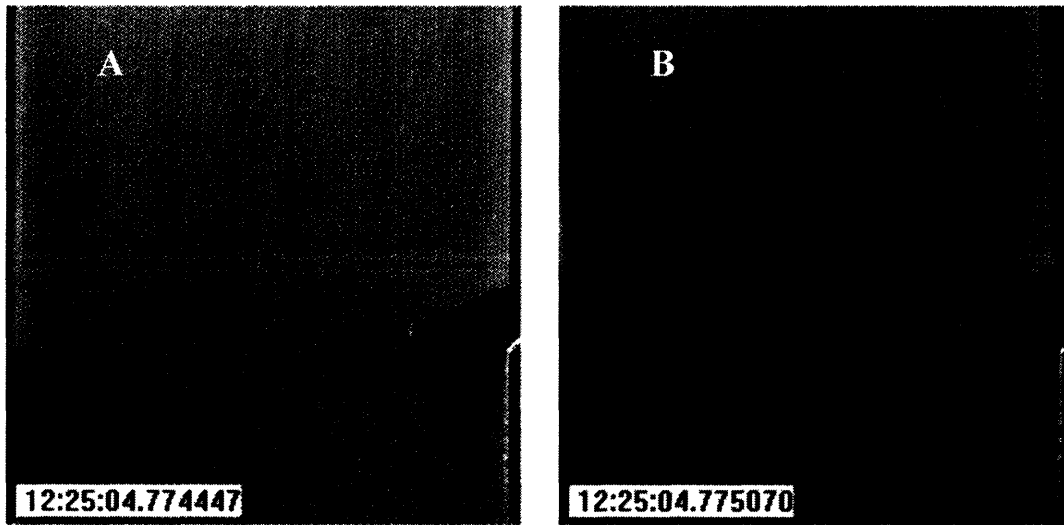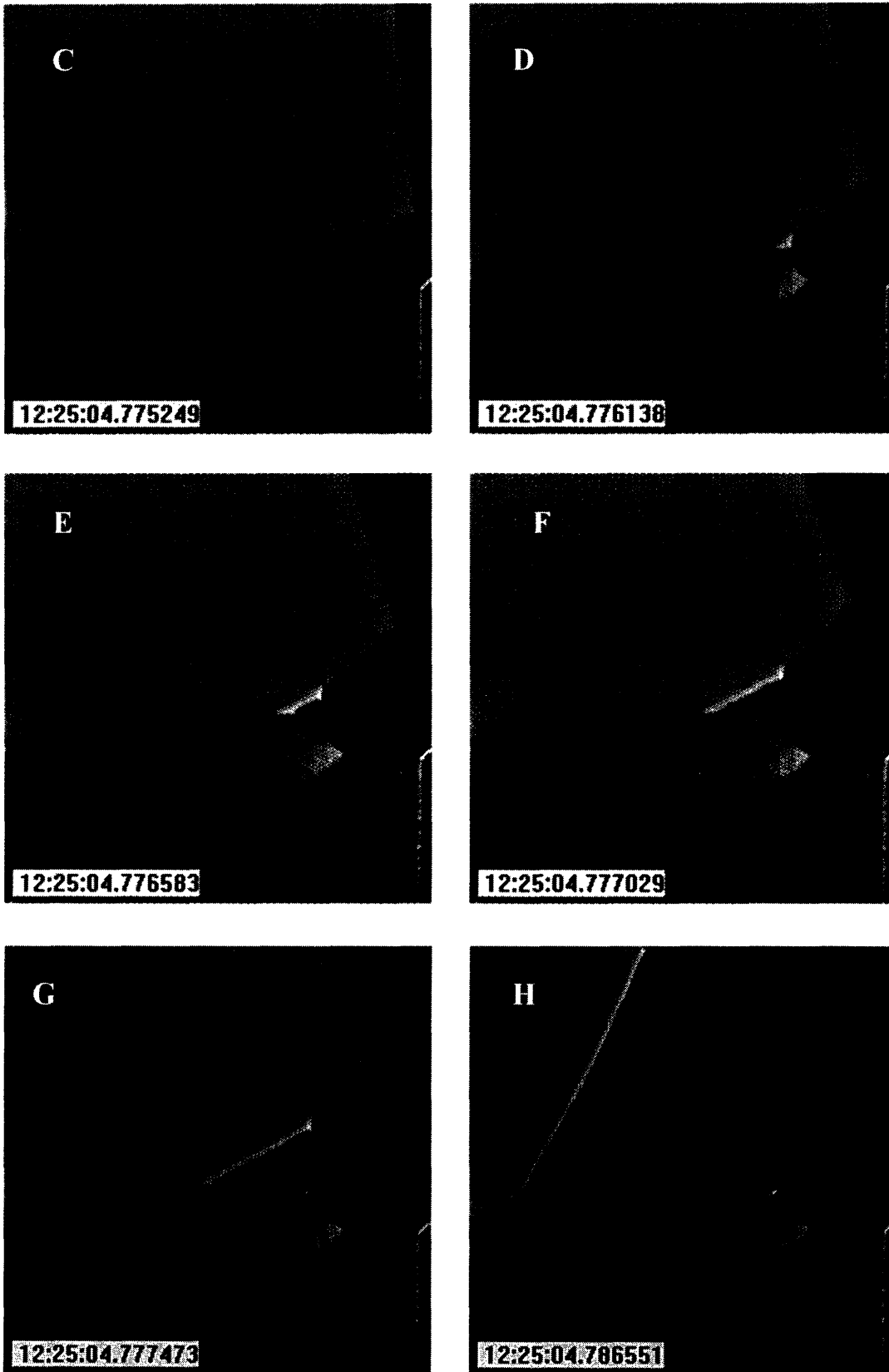
Figure 2.6 Yielding and ripping in Notched Izod impact test of a sample 3.23mm thick.

The specimen deforms a small amount before yielding. Excessive notch blunting is visible from frames **A** through **D** followed by more clearly visible plastically shearing zones at 0.802ms after the pendulum impacts the specimen. At 1.691ms **(D)** a tear starts to form. At 12.104ms the pendulum loses contact with the specimen and the tear stops propagating. The average rate of propagation of the rip once it starts to form is 0.693m/s, over 100 times slower than the crack propagation for the 6.35mm samples.

Most of the fracture energies are within 10% of each other given the same thickness and pendulum weight, however, the fracture energy for N17 was 35% lower than for N16. In Figure 2.7 the first series of six images is of N16 and the second series is of N17. In the higher energy break, yielding occurs evenly on the top and bottom sides of the notch; in the lower energy break, yielding occurs mostly on the bottom portion. Because of a microscopic defect in N17 the top portion begins to rip after almost no yielding. The energy that would normally be used to generate that yielding is therefore not included in the total energy to fracture. These images show the influence of small defects in fracture energy. Figure 2.8 shows the notches for N16 and N17, there are no major differences visible between them. They each have a radius of 6μm and their angles are only off of each other by half a degree.

A   12:25:04.774447

B   12:25:04.775249

C   12:25:04.776138

D   12:25:04.776583

E   12:25:04.777029

F   12:25:04.777473

(a)

27
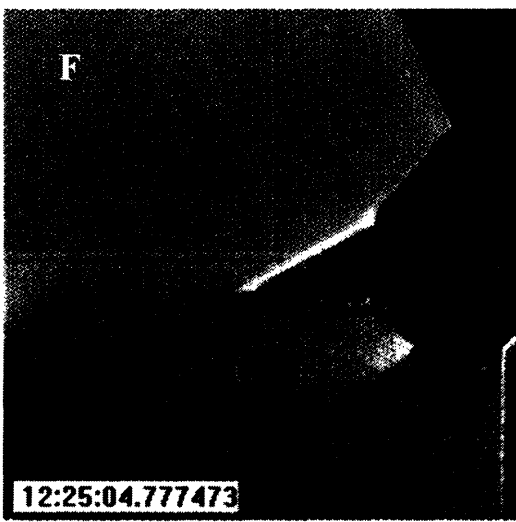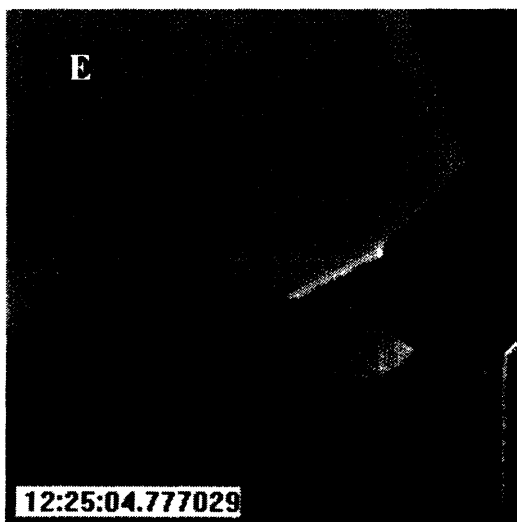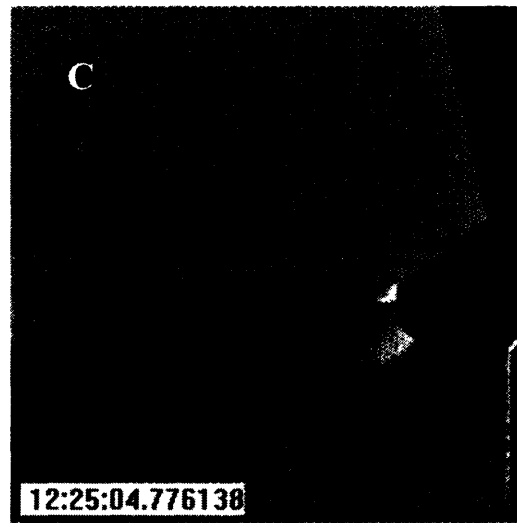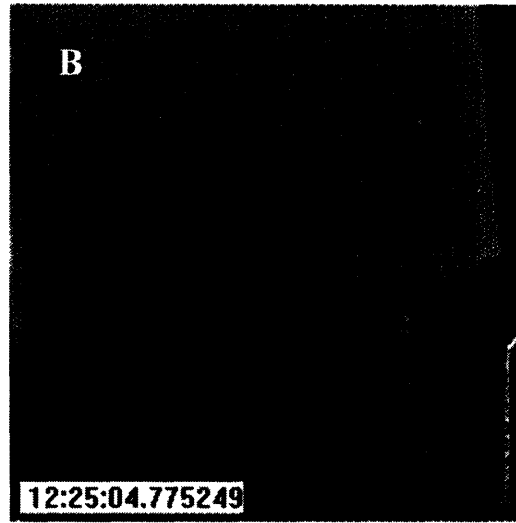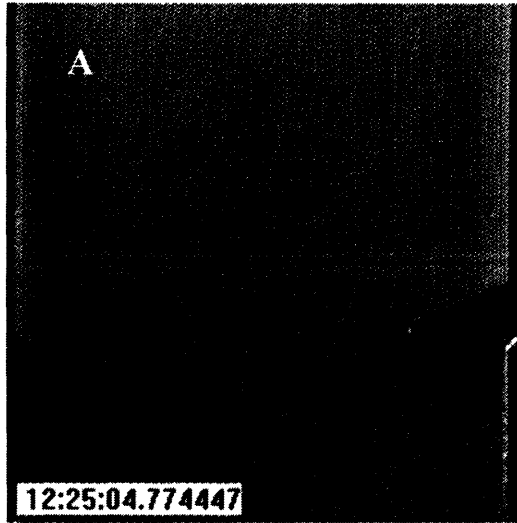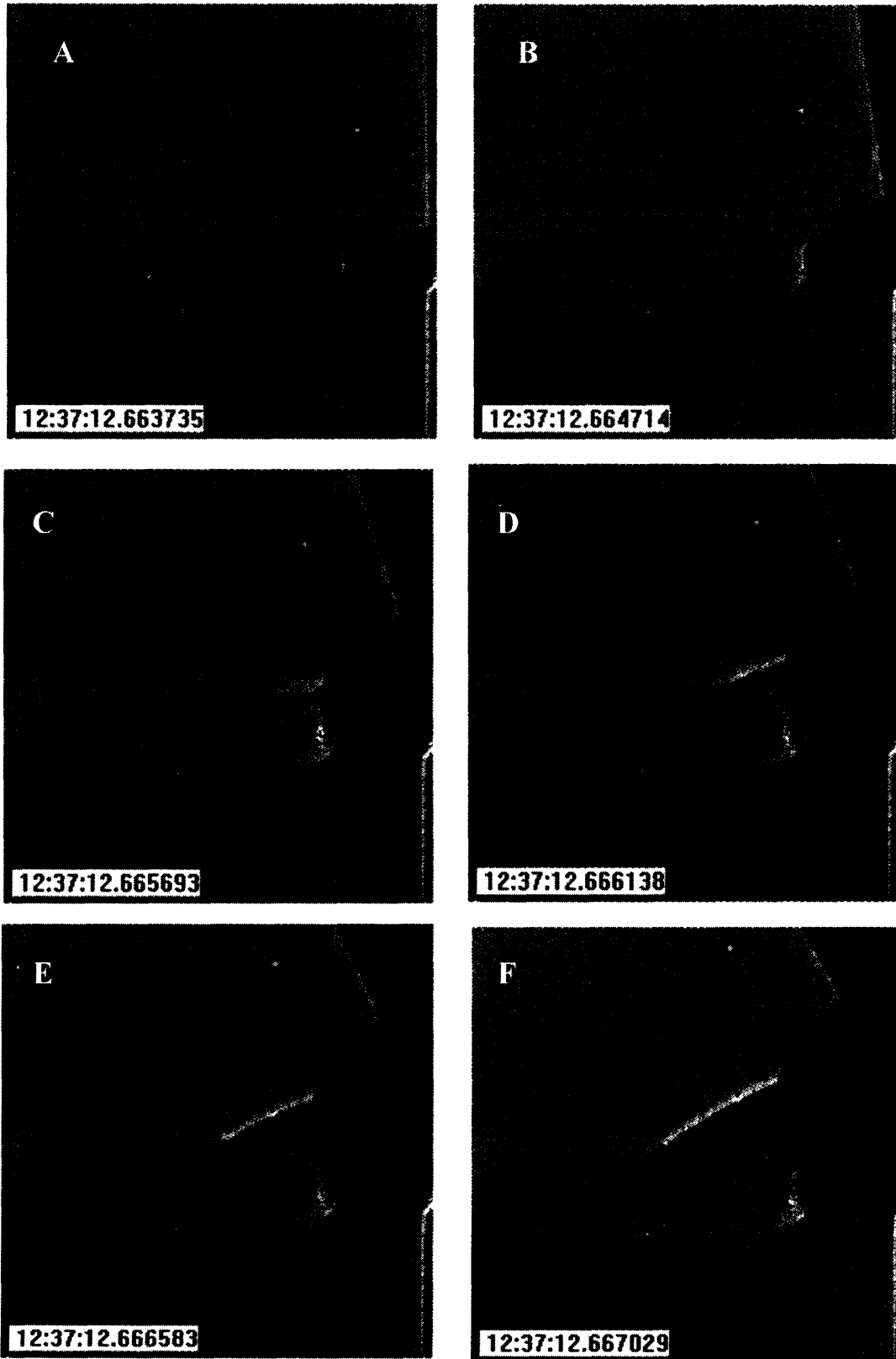
Figure 2.7 Yielding and ripping for Notched Izod impact test of two 3.23mm thick specimens with fracture energies varying by 35%. a) 898 J/m, b) 860.29 J/m
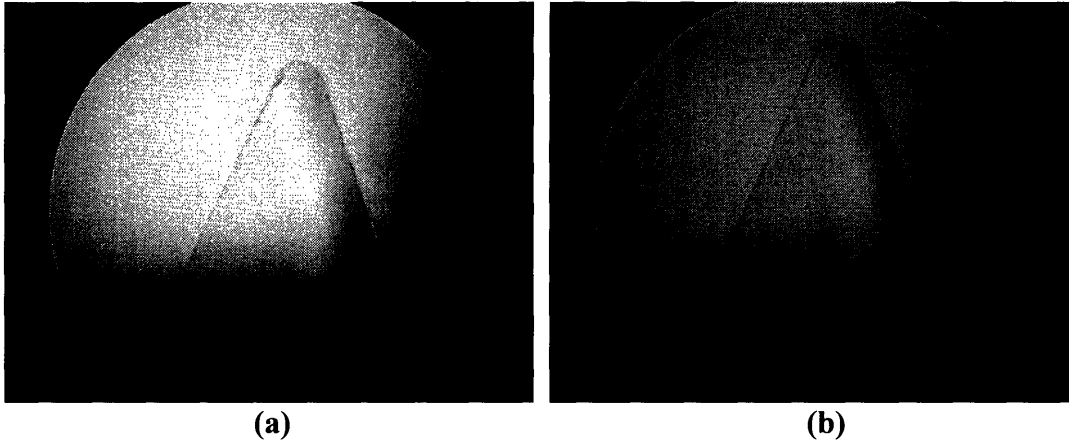
(a)   **(b)**

Figure 2.8 Images of notches for the two specimens shown in Figure 2.7. **a)** N16 **b)** N17

2.3.2 Quasi-Static Izod Results and Discussion

Figure 2.9 below shows the results for one of the Quasi-Static tests of the 6.35mm thick specimens and for the test of the 3.23mm thick specimen that was bent the furthest. The shapes of the curves within each thickness are nearly identical with the 3.23mm results extending to different distances depending on how long the test was run. Results for all Quasi-Static test runs are in Appendix B. The maximum force and the fracture energy for each run are listed in Table 2.3.
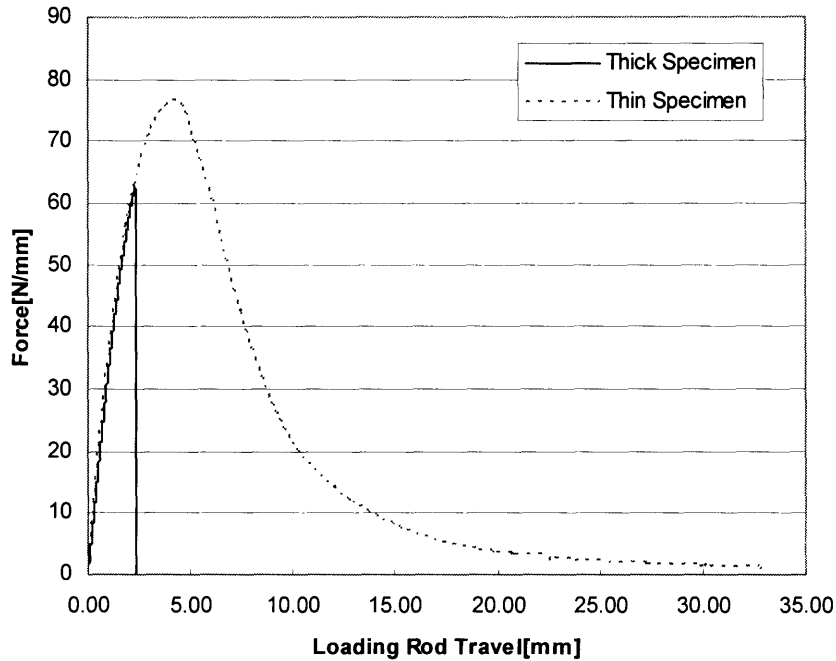
Figure 2.9 Typical results for Quasi-Static Izod testing for 3.23mm and 6.35mm thick specimens.

29

Table 2.3 Maximum force and fracture energy per thickness reached by each sample.

Thickness (mm)	Maximum Force(N)	Fracture Energy per Thickness (J/m)
6.35	399.79	81.35
6.35	413.48	82.7
6.35	421.48	86.3
6.35	395.98	72
3.23	243.29	500.5
3.23	258.69	518.7
3.23	252.53	611.5
3.23	251.86	611.9
3.23	247.77	619.7
3.23	263.38	633.8
3.23	256.98	617.9

The fracture energies for the Quasi-Static tests are less than for the Notched Izod Impact tests due to the lower speed, but the trend of reduction in fracture energy from thin to thick samples is the same. The thin specimen fracture energy per width is approximately seven times that of the thick specimen for both Notched Izod impact and Quasi-Static testing. This was expected from the similarity in fracture progression between the Notched Izod impact and Quasi-Static tests. The thick specimens yielded slightly followed by failure in a brittle manner. The thin specimens yielded extensively and then fractured by tearing. As in the Notched Izod impact test, the thin specimens did not tear completely, but were left with a hinged break.

The 6.35mm specimens underwent brittle fracture at an average force of 64.27N/mm with a standard deviation of 2.9%. The fracture surface was the same as that of the Izod tested specimens of the same thickness.

(a)   (b)
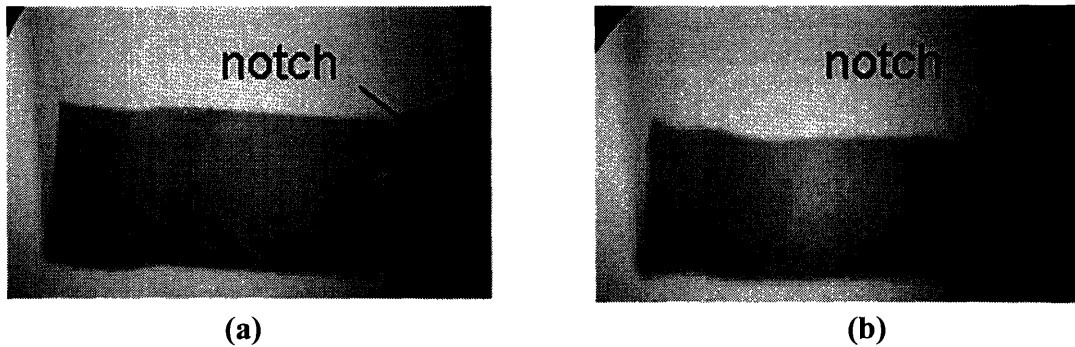
Figure 2.10 Fracture surface of 6.35mm thick sample for **(a)** Quasi-Static Izod **(b)** Notched Izod impact

The fracture was instantaneous. Figure 2.11 shows an image taken every 25 seconds during the test as well as one immediately before and after the fracture.
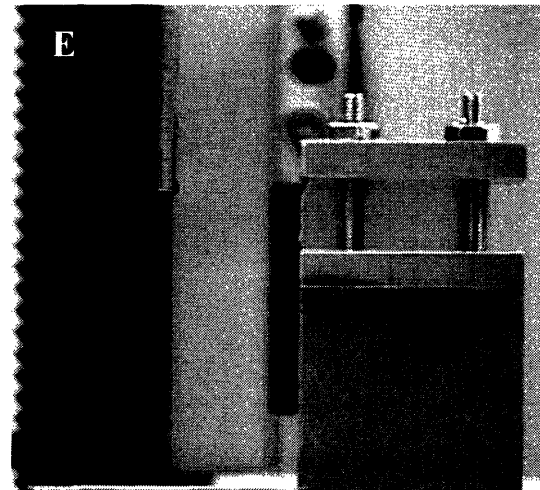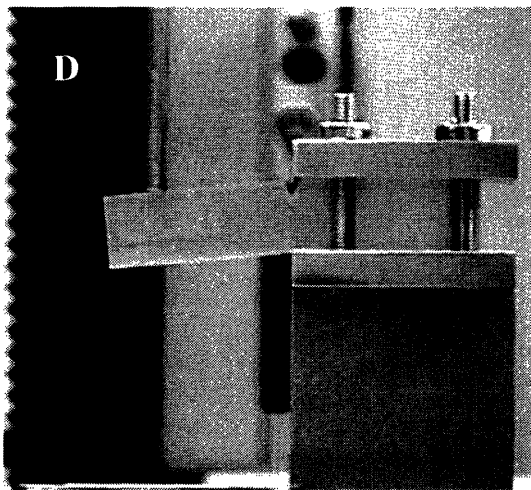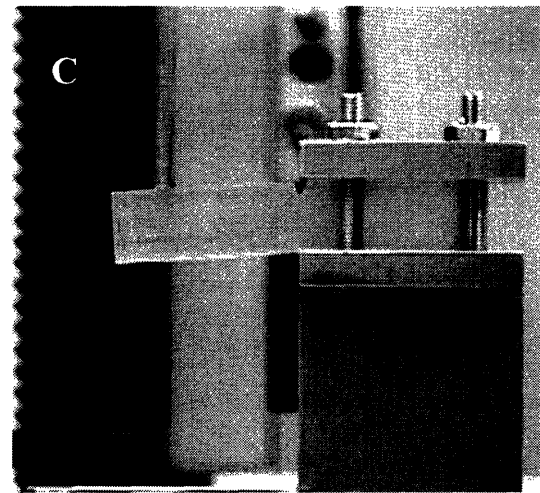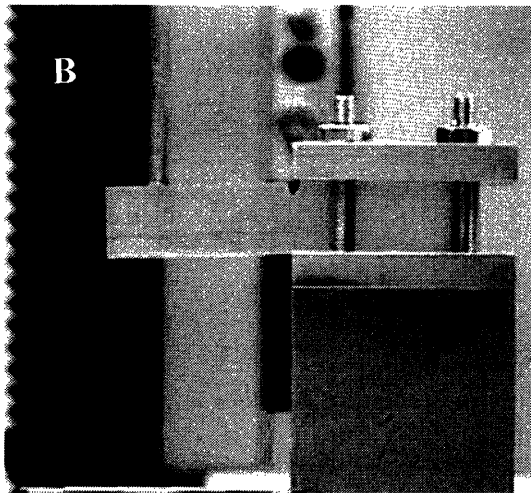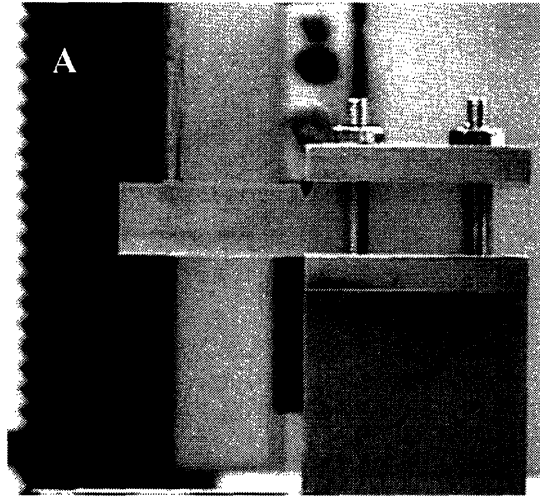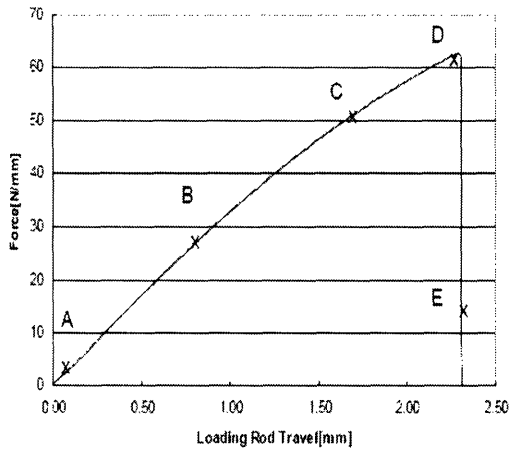
Figure 2.11 Images from a Quasi-Static Izod test of 6.35mm thick specimen.

There is no sign of cracking or yielding past the immediate crack tip region prior to the final fracture. The fracture occurs 70 seconds into the test when the loading rod has traveled 2.33 mm vertically. In another test of a specimen of the same dimensions in

which the camera was placed closer and the image was magnified, there is a small amount of yielding visible just at the crack tip. The series of magnified pictures is shown in Figure 2.12 below.
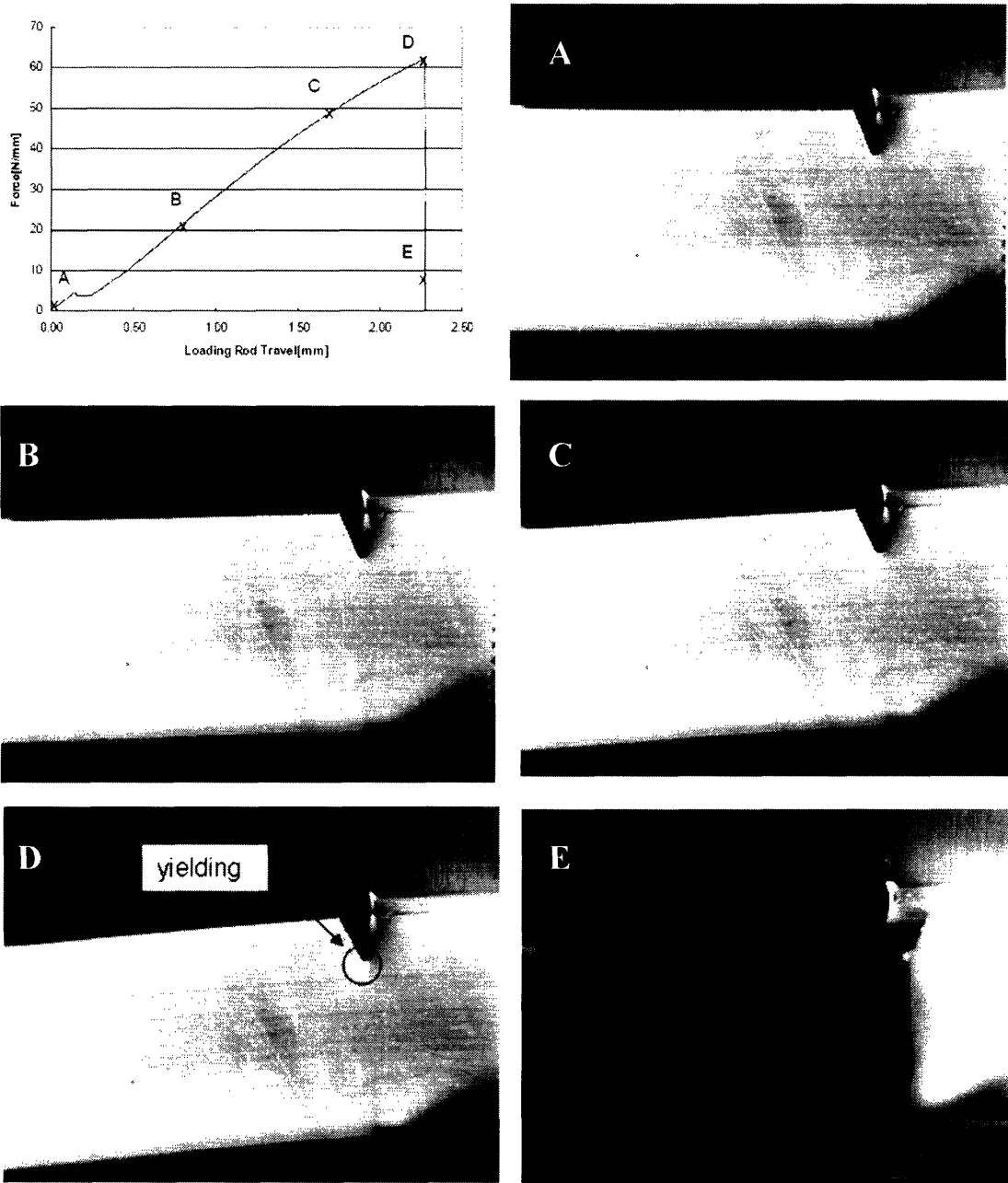
Figure 2.12 Magnified images of Quasi-Static Izod test of 6.35mm thick specimen.

The 3.23mm specimens reached an average maximum force of 74.9N/mm with a standard deviation of 2.7%. At the maximum force the entire width began to yield in the area near the crack tip. Because of the decreased slope of the plastic regime of the characteristic stress-strain curve for polycarbonate, the force required for further deformation decreases. Shortly after yielding initiated a rip begins to form. The yielding and tearing then progress down the depth of the specimen, propagating the gap. Figure

32

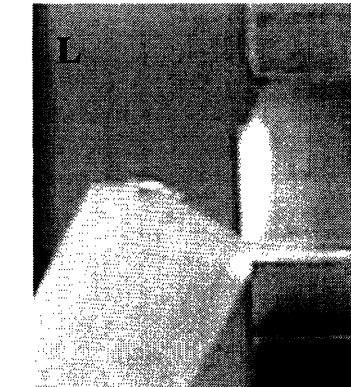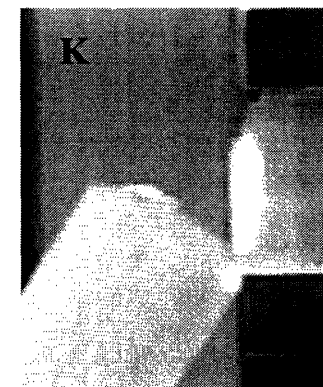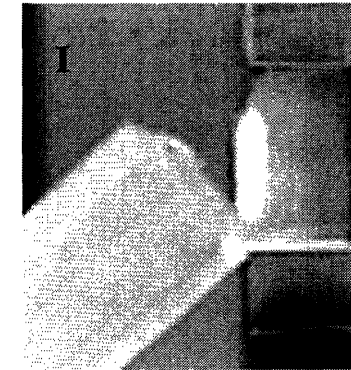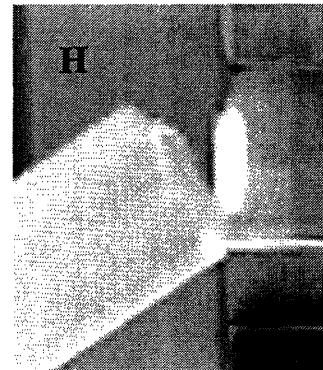2.13 shows images taken during the test as well as the force-loading rod travel curve for the thin specimen.

(a)

(b)
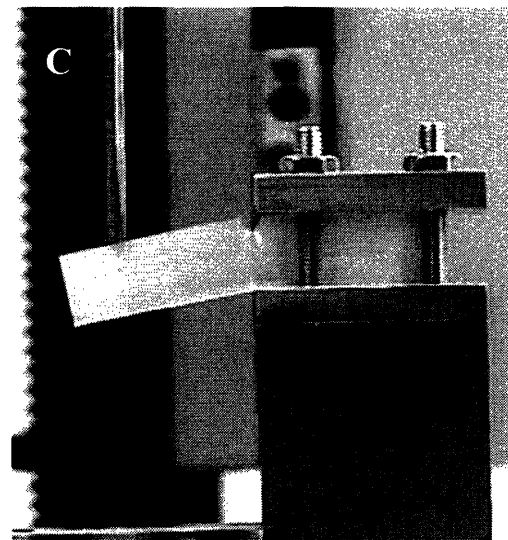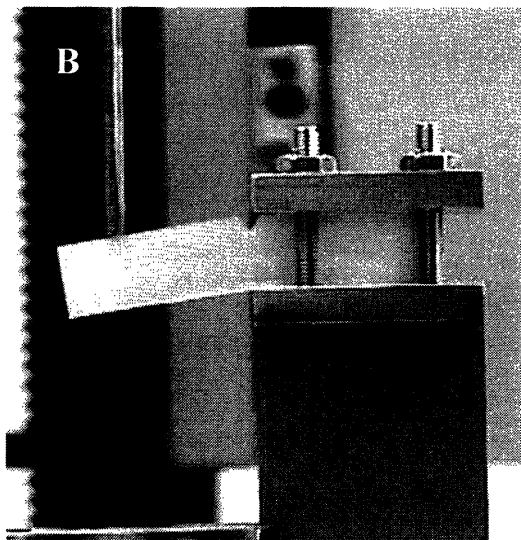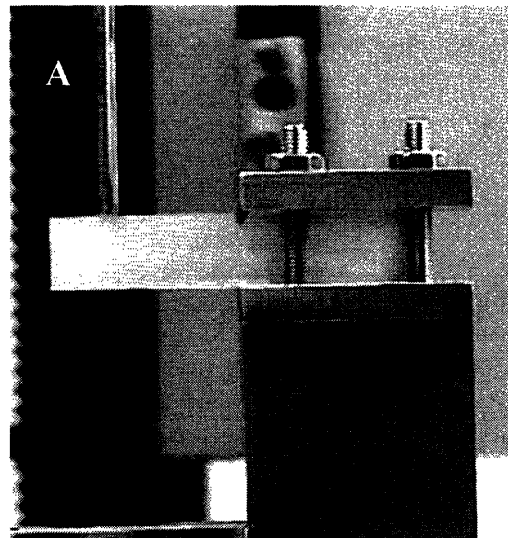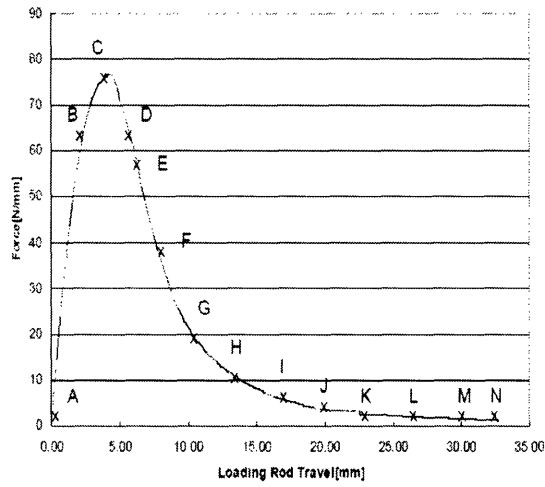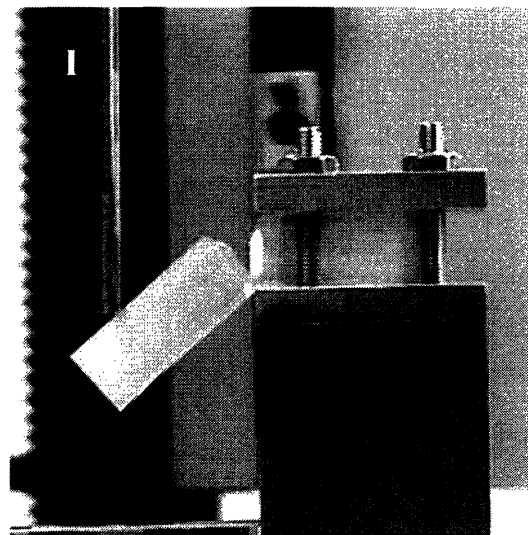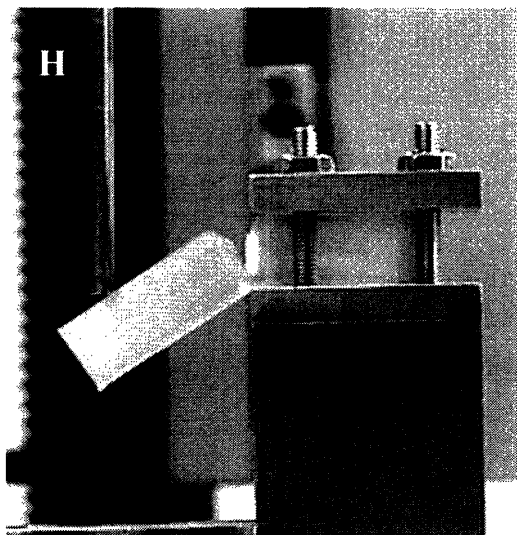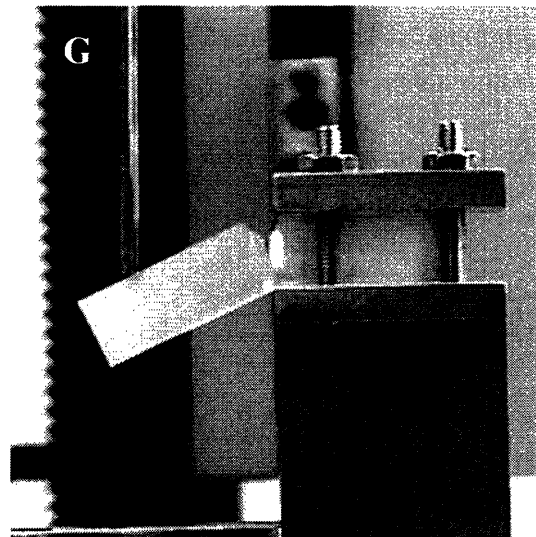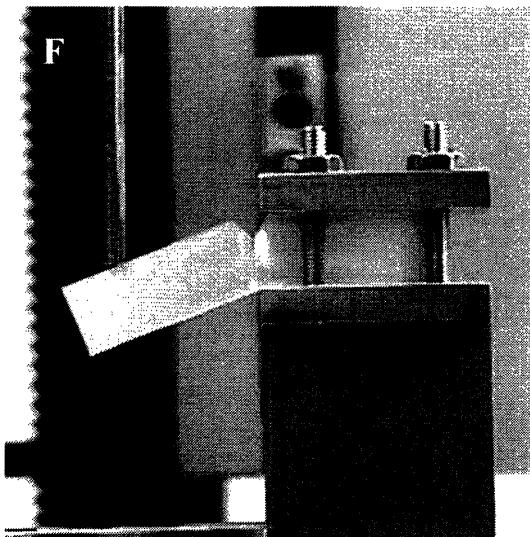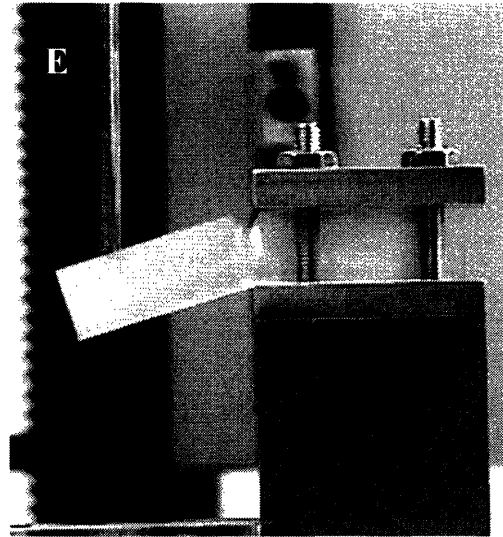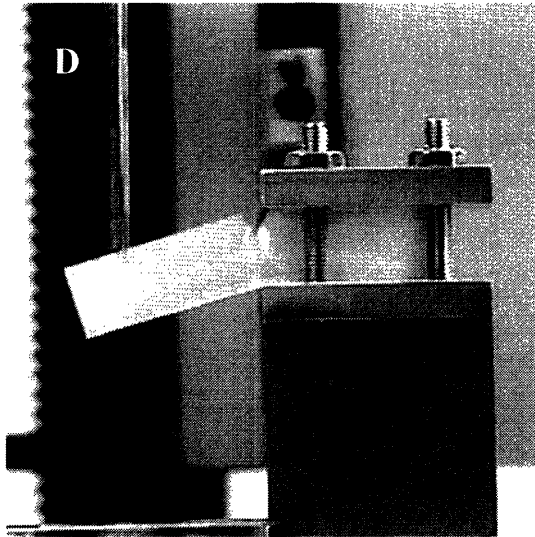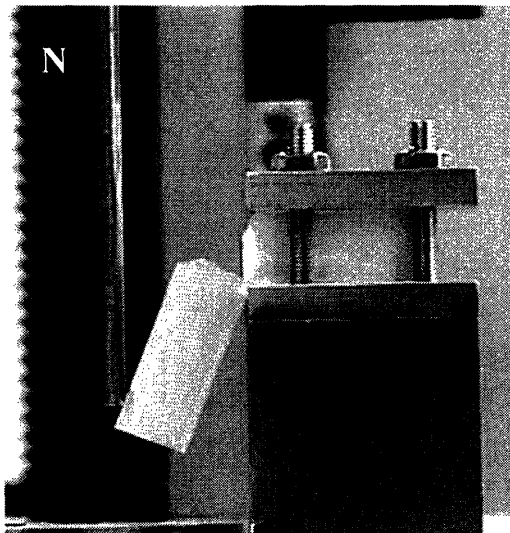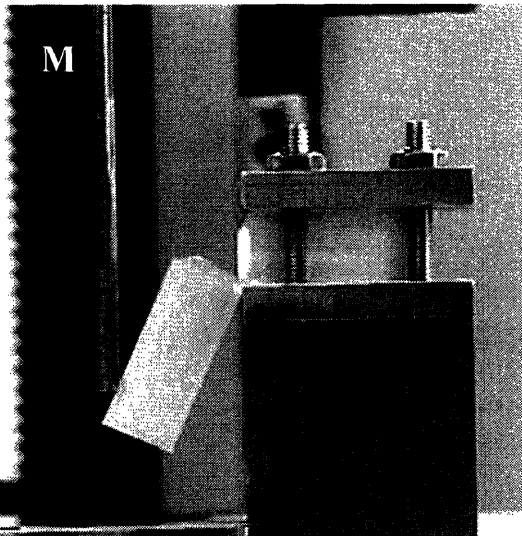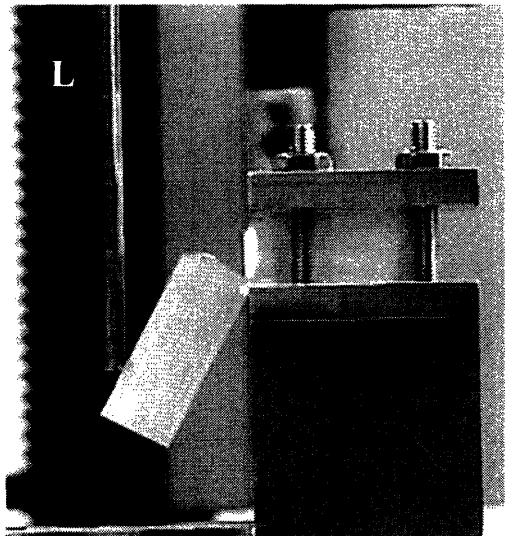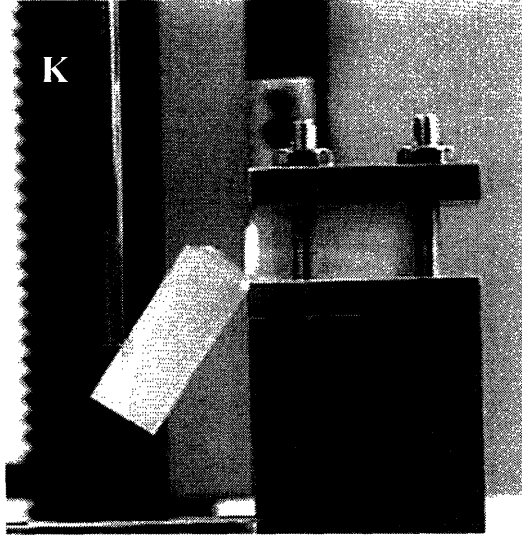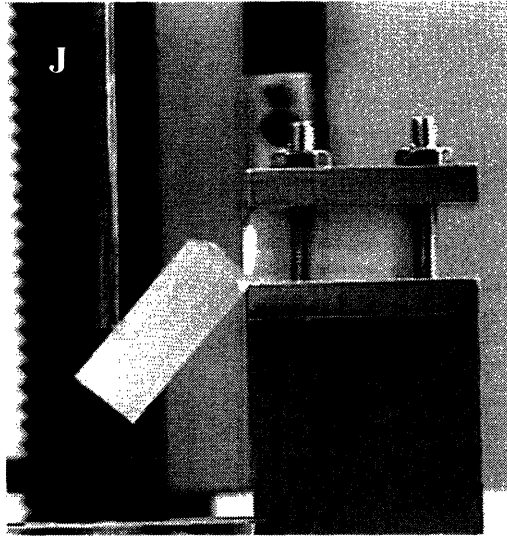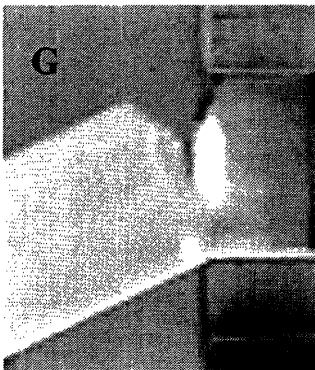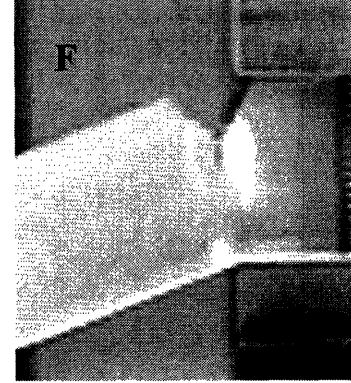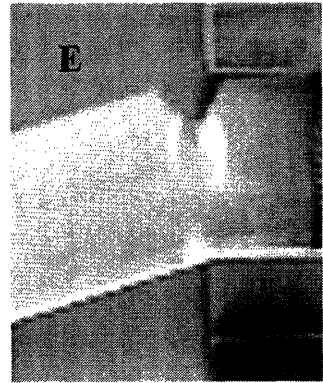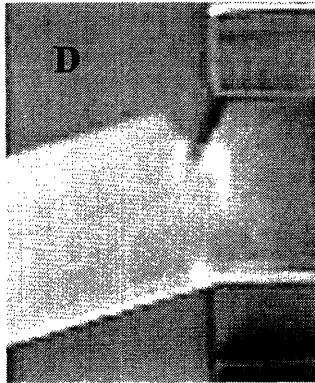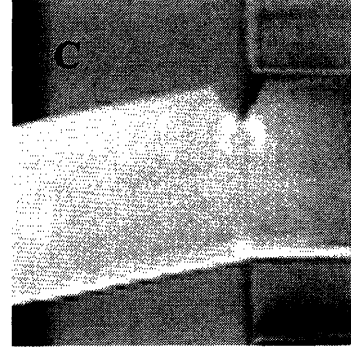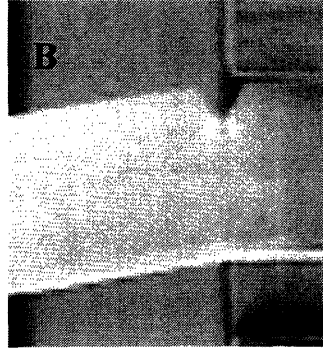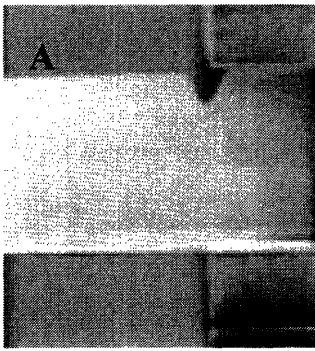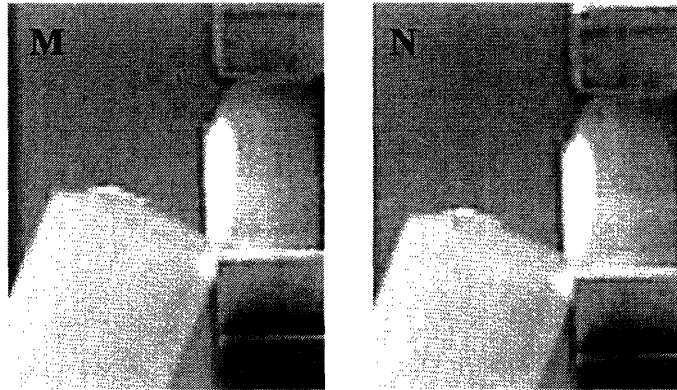
Figure 2.13 Images from Quasi-Static Izod test of a specimen 3.23mm thick. **a)** wide view **b)** enlarged view of notch

The yielding is visible through the whitening of the polycarbonate. It occurs simultaneously at the crack tip and at the bottom edge of the specimen at the corner of the clamp at a force of 248N when the loading rod has traveled 4.62mm. However as the loading rod continues moving, the yielding region near the crack tip expands while that at the base remains the same size. The specimen begins to tear at the crack tip at a loading rod travel of 6.37mm. The specimen continues to gradually tear until it hinges on a small fraction of its depth. The force asymptotically approached zero as the loading rod serves only to push the unconstrained half of the specimen closer to a 90° angle with the clamped half, rather than causing any further tearing the hinged ligament continues to undergo more plastic deformation. When the loading rod was lifted, the specimen had some immediate elastic recovery. For this sample the maximum angle reached between the bottom surface of the "free" and the horizontal was 65°, after removal of the indenter it recovered to 54°. A picture of the specimen before and after elastic recovery is in Figure 2.14 below.


(a)   **(b)**
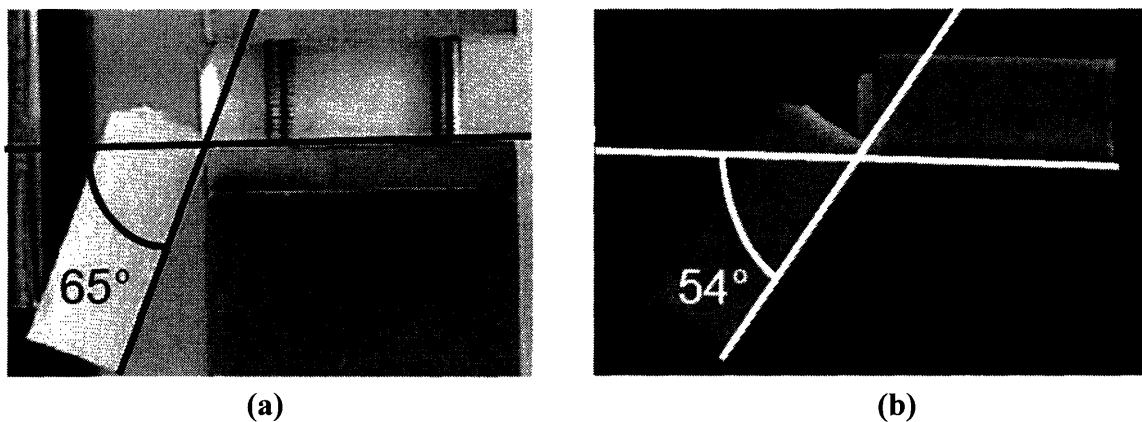
Figure 2.14 Elastic recovery of 3.23mm thick specimen after Quasi-Static Izod testing. **a)** before recovery **b)** after recovery

Nearly identical behavior was seen on a test done on a specimen of the same thickness with the camera closer to the specimen and the image magnified.
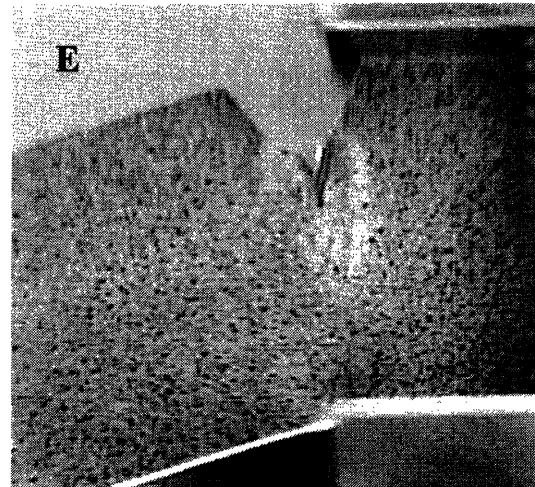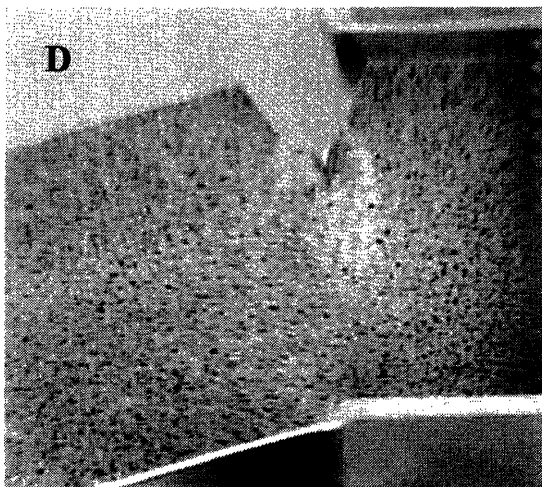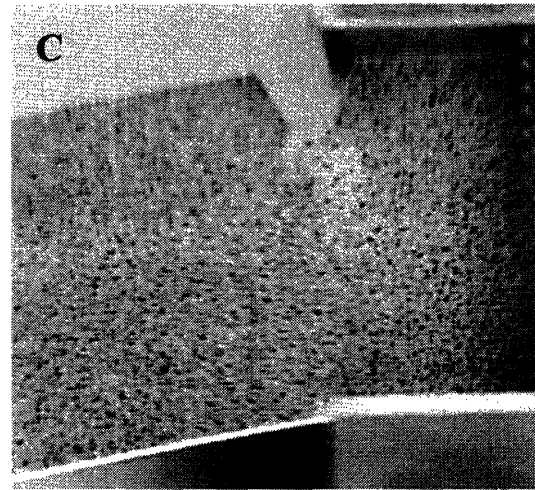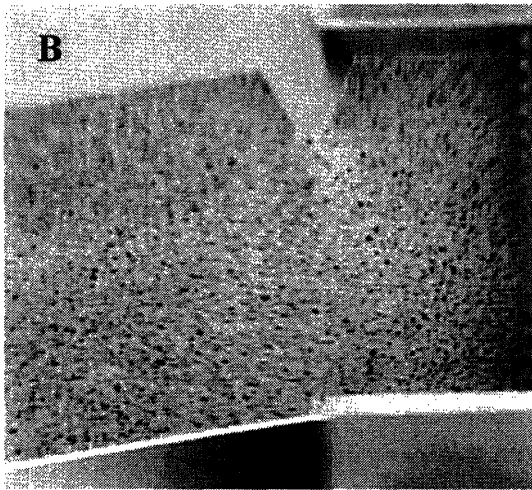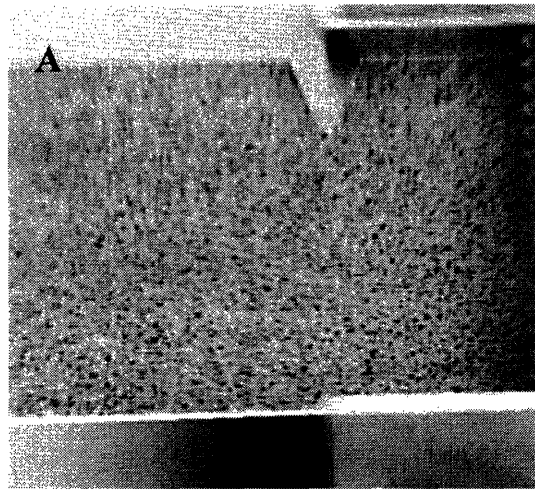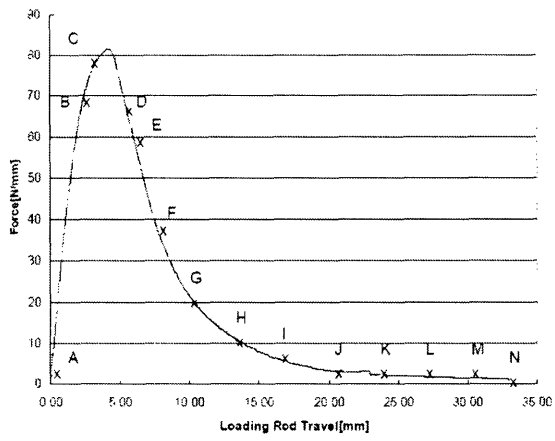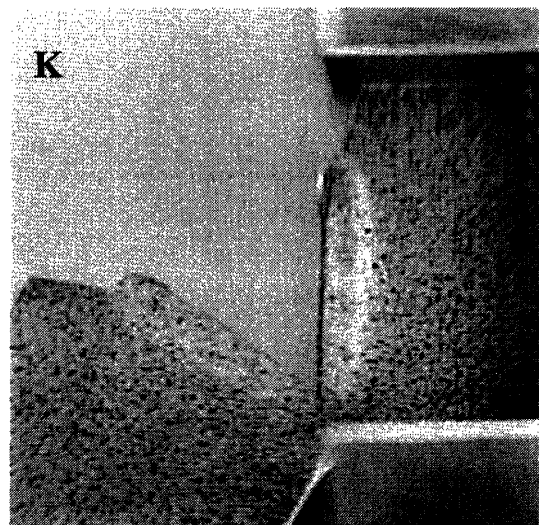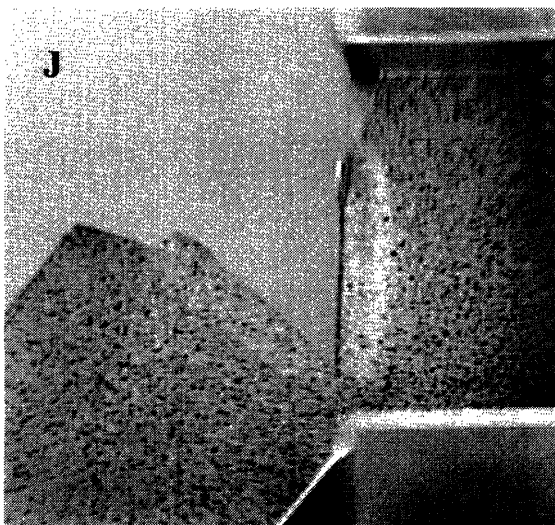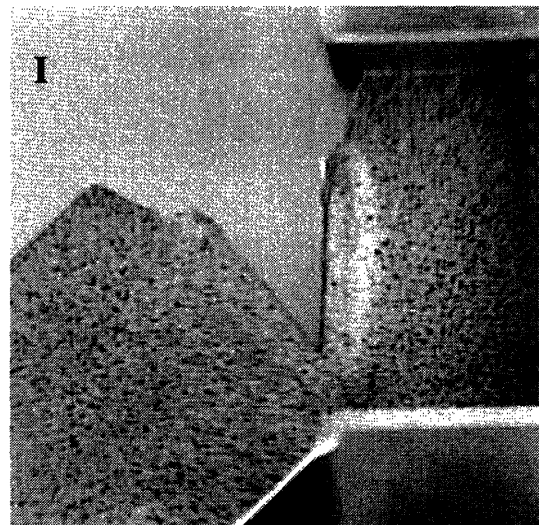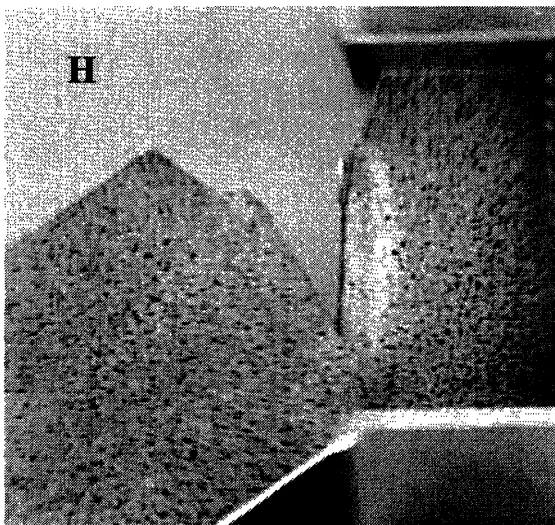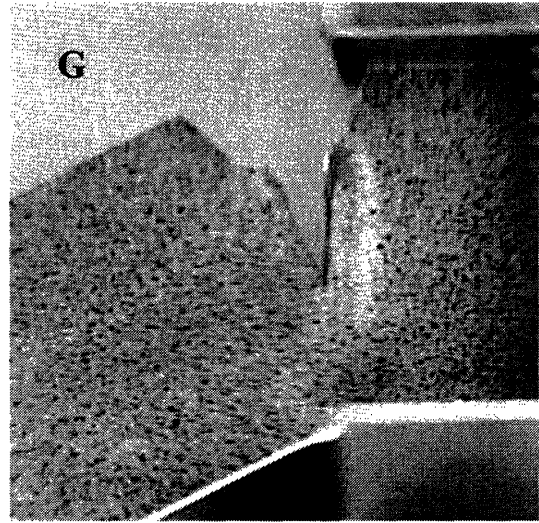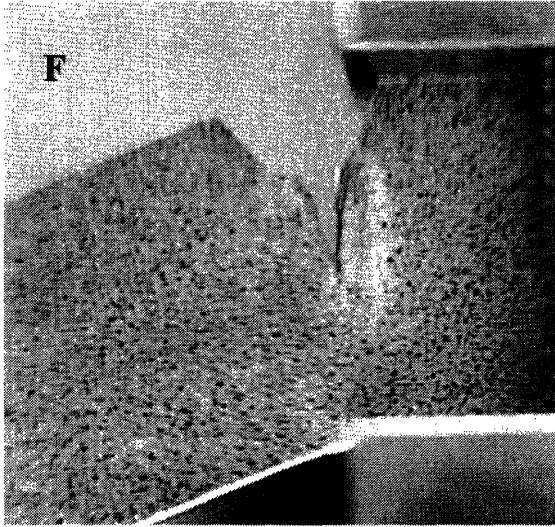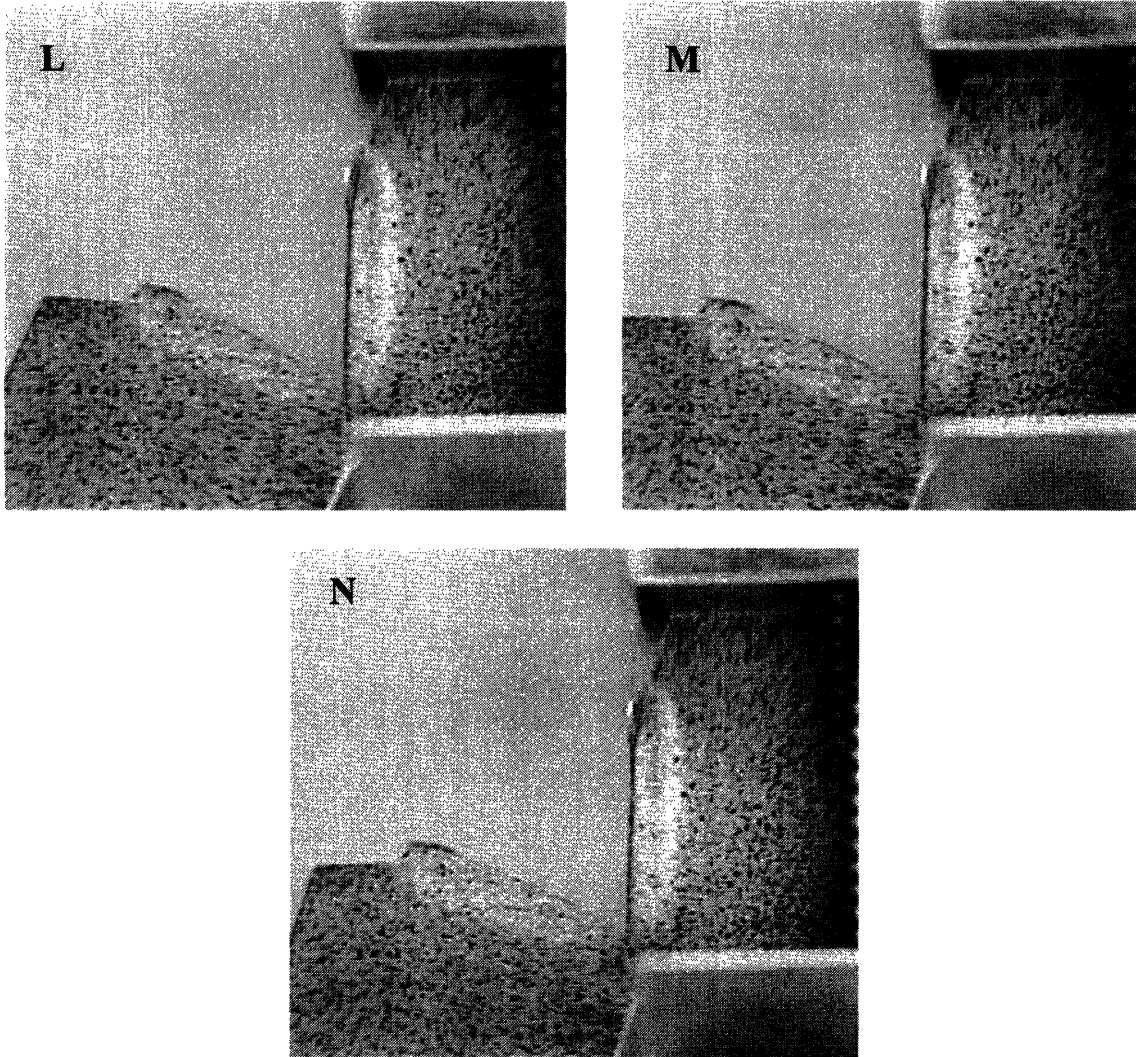
Figure 2.15 Magnified image of deformation of 3.23mm thick specimen in Quasi-Static Izod test.

Yielding begins when the loading rod has traveled 4.03mm**(C)**. Tearing begins at a loading rod travel of 6.07mm**(D)** And the test ends with a hinged break at 33mm**(M)** with shear bands the full depth of the sample on both sides of the notch. One aspect of this fracture progression which is not consistent with the high speed impact testing is the location of the tear relative to the centerline of the notch. In each of the Quasi-Static tests the tear initiates and propagated down the center; in each of the impact tests the tear occurs in the upper portion of the notch as shown in Figure 2.16.
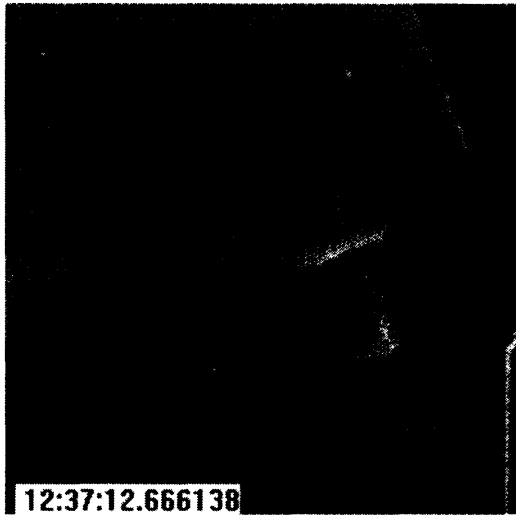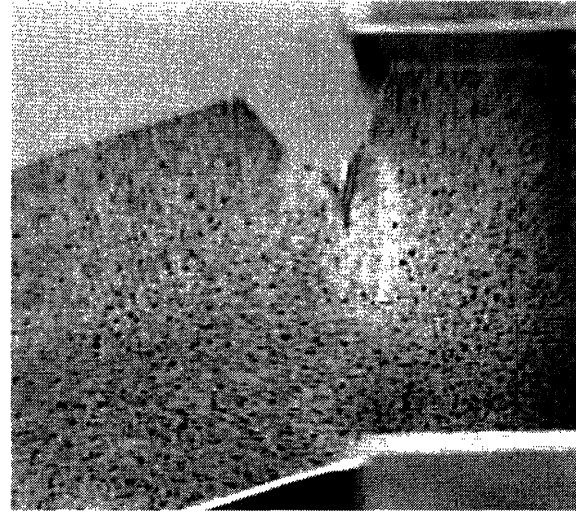
(a)   **(b)**

Figure 2.16 Comparison of tear location in Notched Izod impact and Quasi-Static Izod testing of 3.23mm thick specimens. **a)** Notched Izod impact **b)** Quasi-Static

Chapter Three: Modeling

3.1 Introduction

The finite element simulation program Abaqus was used to create a three dimensional model of the specimen for the Notched Izod impact testing. Abaqus explicit was chosen over Abaqus standard because of its effectiveness at solving highly nonlinear dynamic problems with failure.

3.2 Material Model

The constitutive model used is a three-dimensional model which accounts for rate, temperature, and pressure dependent deformation of thermoplastic materials. The model was first created by Boyce et al.(1988) and Arruda and Boyce(1993a,b) and updated to account for high rate and low temperature loading by Mulliken and Boyce(2004). The model has been validated for PC (Arruda and Boyce, 1993a, Boyce et al., 1994) and PMMA (Boyce et al., 1988, Arruda et al., 1995) for plane strain compression, simple shear, uniaxial tension, and uniaxial compression at low to moderate strain rates(10^{-3} s^{-1} to 1 s^{-1}) and temperatures from 300 K to 363 K. The model was modified by Mulliken and Boyce (2004) include secondary molecular relaxation aspects of polymeric material structure/mobility and then shown to accurately predict uniaxial compression of PC at high strain rates (5050 s^{-1}) .

The current model consists of five components: two linear elastic springs, two viscoplastic dashpots, and a non-linear Langevin spring. Each linear elastic spring acts in series with a viscoplastic dashpot, and the spring-dashpot pairs act in parallel with the non-linear spring. The model assumes that the resistance to deformation of thermoplastic materials can be decomposed into intermolecular resistance to chain-segment rotation represented by the elastic springs and viscoplastic dashpots, and entropic resistance to chain alignment represented by the Langevin spring. The intermolecular resistance is decomposed into two rate-activated processes, one associated with the primary (α) process and one associated with the most significant secondary (β) process. A one dimensional depiction of the model is shown in Figure 3.1.
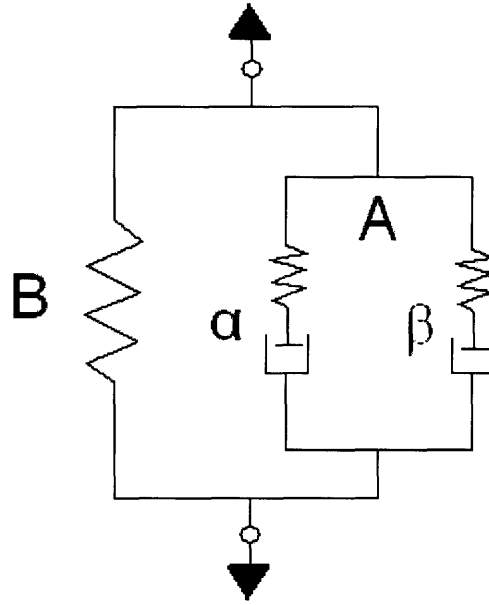
Figure 3.1 One dimensional depiction of constitutive model for rate-dependent thermoplastic behavior.

The α and β-components have unique material parameter definitions which vary with temperature and strain rate, so that their relative importance varies with temperature and strain rate as well. The β-component is fairly compliant and weak at high temperatures and low strain rates and restricted, providing stiffness and resistance to yielding, at low temperatures and high strain rates. Consequently, at high temperatures and low strain rates only the α-component will be visible, but at low temperatures and high strain rates polycarbonate's behavior will be a function of the sum of the two molecular-level motion resistances.

The stress tensors for the α and β spring and dashpot networks are related to the strain by the constitutive laws for the linear elastic springs:

$$\mathbf{T}_{Ai} = \frac{1}{J_i} L_i^e \left[\ln \mathbf{V}_{Ai}^e \right]$$ [3.1]

where $\mathbf{T}_{Ai}$ ($i = \alpha, \beta$) is the Cauchy stress tensor; J_i is the elastic volume change; L_i^e is the fourth-order modulus tensor; and $\ln \mathbf{V}_{Ai}^e$ is the Henky Strain. The modulus tensors can be derived from any two component-specific elastic constants, such as the shear modulus and bulk modulus.

The stress tensor for the non-linear Langevin spring component is defined using the Arruda-Boyce 8-chain interpretation of molecular alignment:

$$\mathbf{T}_B = \frac{nk\theta}{3} \frac{\sqrt{N}}{\lambda^p_{chain}} L^{-1}\left(\frac{\lambda^p_{chain}}{\sqrt{N}}\right)\overline{\mathbf{B}'_B} \qquad [3.2]$$

$$L(\beta) \equiv \coth\beta - \frac{1}{\beta} \qquad [3.3]$$

$$\overline{\mathbf{B}'_B} = \left(\det\mathbf{F}\right)^{-2/3}\mathbf{F}\mathbf{F}^T \qquad [3.4]$$

where n is the number of chains per unit volume, k is Boltzmann's constant, θ is the absolute temperature, $\sqrt{N}$ is the limiting chain extensibility, λ^p_{chain} is the stretch on a chain in the eight-chain network; L is the Langevin function, $\overline{\mathbf{B}'_B}$ is the deviatoric part of isochoric left Cauchy-Green tensor, and $\mathbf{F}$ is the deformation gradient.

The total stress is the sum of all three stress tensors.

$$\mathbf{T} = \mathbf{T}_{A\alpha} + \mathbf{T}_{A\beta} + \mathbf{T}_B \qquad \overline{\mathbf{B}'_B} = \left(\det\mathbf{F}\right)^{-2/3}\mathbf{F}\mathbf{F}^T \qquad [3.5]$$

The constitutive law for the α and β viscoplastic behavior is:

$$\dot{\gamma}^p_i = \dot{\gamma}^p_{0,i}\exp\left[-\frac{\Delta G_i}{k\theta}\left(1 - \frac{\tau_i}{s_i + \alpha_{p,i}p}\right)\right] \qquad [3.6]$$

where $\dot{\gamma}^p_i$ is the plastic strain rate, $\dot{\gamma}^p_{0,i}$ is the pre-exponential factor proportional to the attempt frequency, ΔG_i is the activation energy, τ_i is the equivalent shear stress, p is the pressure, $\alpha_{p,i}$ is the pressure coefficient, and s_i is the athermal shear strength.

A full derivation of the model is available in Mulliken and Boyce (2004).

3.3 Notched Izod Impact Model Details

The specimen geometry was discretized with the three-dimensional linear element ABAQUS type C3D8R. This is a three-dimensional linear displacement interpolation continuum element defined by 8 nodes. A continuum element is a basic solid element that can be used for both linear analysis and non-linear analysis involving contact, plasticity, and large deformations. The "R" means that reduced integration is used; there is one integration point at the center of each element from which the position of each node of the element is calculated. ABAQUS Explicit code requires using reduced integration. The reduced integration can lead to problems with zero energy (hour glassing) modes and requires some hour glass control to be used in conjunction with the elements.

The pendulum was modeled by a rigid surface 2mm high and 8mm wide with curved ends centered at 22mm above the midpoint of the specimen. The surface was defined as a contact pair with the portion of the specimen 17mm to 27mm above the notch. It was assigned a reference point with a mass of 0.456kg equal to that of the pendulum. The reference point was given an initial velocity in the horizontal direction of 3.46m/s, the speed at which the pendulum hits the specimen.

The geometry and boundary constraints of the model were identical to that of the specimen. To reduce the simulation run time, symmetry was assumed about the plane halfway through the width of the sample. That center plane was then constrained from moving in the direction normal to the plane. The rest of the boundary conditions were imposed to simulate the restrictions placed on the specimen during the Izod test. The bottom half of the right and left surfaces were constrained in all three translational directions and all three rotational directions. The notch was modeled using an average dimension from the notches measured for the experimental portion rather than that of the standard.
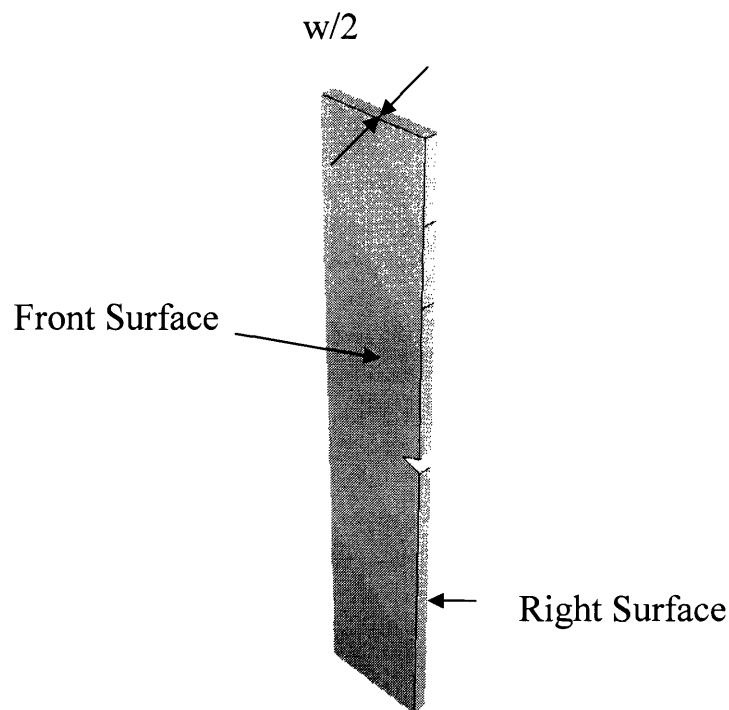
Figure 3.2 Picture of Notched Izod model geometry.

The front plane of the mesh has five distinct regions as shown in Figure 3.3. The lower third **(A)** has the coarsest mesh as it is constrained and does not undergo any significant stresses or deformation. The upper third **(B)** that is not a part of the contact surface has the next coarsest mesh. This region has more freedom of movement than the bottom region, but is still not a concentration point for stresses. The region parallel with the contact surface **(C)** is significantly more refined in order to guarantee good contact with the pendulum since contact can only be made at the nodes. The region around the notch

(D) is the most refined since that is where the stress is concentrated in the Izod's three-point bending state. There are 11 elements along the circumference of the semicircle of the notch and an additional 11 elements along each edge of the notch. A combination of a semicircular and fanning pattern was used to transition from the rounded notch to the rectangular border of the specimen. There are eight elements through the thickness of the specimen to accurately model the transition from plane stress to plane strain that determines the ductility of the fracture.
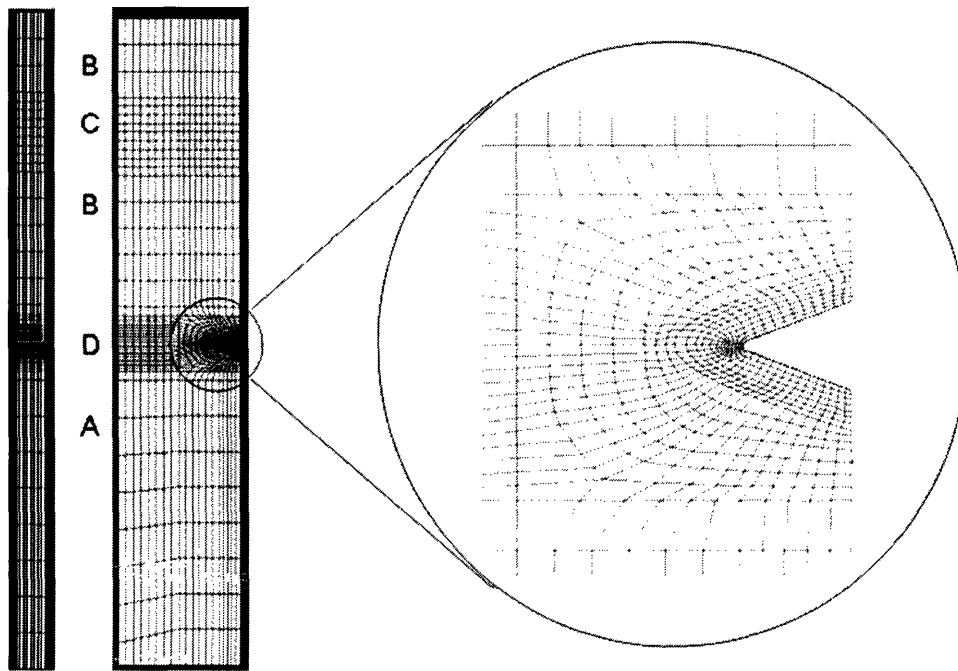
Figure 3.3 Picture of mesh from front and side and enlarged picture of the region around the notch.

3.4 Notched Izod Impact Model Results

Thin (3.23 mm thick) Specimen:
The results for the model of the thin (3.23mm thick) specimen are shown in Figures 3.4 through 3.8 below. Figure 3.4 shows a series of Mises stress contours for the outside surface of the specimen from the time the rigid surface impacts it to after tearing has initiated. The Mises stress provides a scalar equivalent stress measure that can be used to assess if the stress levels are high enough to be yielding and plastically deforming the material. First, note that the stress at the impact location is more than an order of magnitude smaller than the highest stress levels that occur at the notch tip region. Notice how that once the transient stresses from the impact settle down, symmetric bands form around the notch tip. The magnitudes of the stresses are only slightly greater on the mid-plane than on the outside surface (due to the nearly plane stress nature of the deformation of this thin specimen) and have the same shapes. In addition to the plastically deforming bands or lobes that form and propagate from the notch tip, a small plastic deformation region is also observed on the compressive side of the bend.

A   B   C
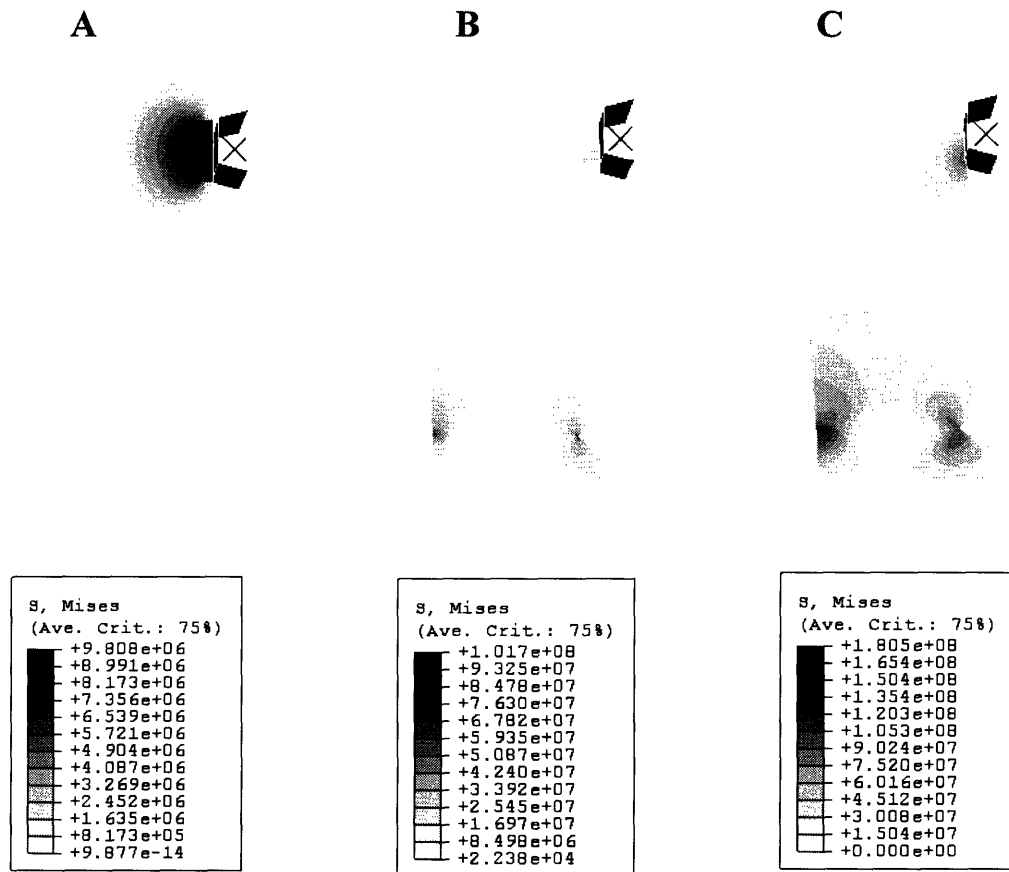


```
S, Mises
(Ave. Crit.: 75%)
    +9.808e+06
    +8.991e+06
    +8.173e+06
    +7.356e+06
    +6.539e+06
    +5.721e+06
    +4.904e+06
    +4.087e+06
    +3.269e+06
    +2.452e+06
    +1.635e+06
    +8.173e+05
    +9.877e-14
```

```
S, Mises
(Ave. Crit.: 75%)
    +1.017e+08
    +9.325e+07
    +8.478e+07
    +7.630e+07
    +6.782e+07
    +5.935e+07
    +5.087e+07
    +4.240e+07
    +3.392e+07
    +2.545e+07
    +1.697e+07
    +8.498e+06
    +2.238e+04
```

```
S, Mises
(Ave. Crit.: 75%)
    +1.805e+08
    +1.654e+08
    +1.504e+08
    +1.354e+08
    +1.203e+08
    +1.053e+08
    +9.024e+07
    +7.520e+07
    +6.016e+07
    +4.512e+07
    +3.008e+07
    +1.504e+07
    +0.000e+00
```

Figure 3.4 Mises stress contours of impact of 3.23mm thick Notched Izod specimen. **A)** at initial impact. **B)** during elastic bending phase **C)** after tearing has initiated

Focusing back on the notch tip where tearing will eventually initiate, Figure 3.5 shows a close-up view of the Mises stress contour around the notch. The blunting of the notch, which was present in both the thick and thin experimental Izod impact tests, is visible in these model results where the yielding of the material in the notch region acts to blunt the notch tip. Also as in the experiment, elliptical shear yielding bands extend out from the notch surface. The magnitude and size of the bands grow with pendulum travel. By Figure 3.5 E, tearing has begun to initiate as indicated by the pocket of zero stress that has formed (there is where the specimen has begun to tear and is no longer bearing load). As the tearing progresses across the width of the specimen, the shear bands follow and indeed begin to travel in a more horizontal manner across the specimen as observed in the experiments on the thin specimens.
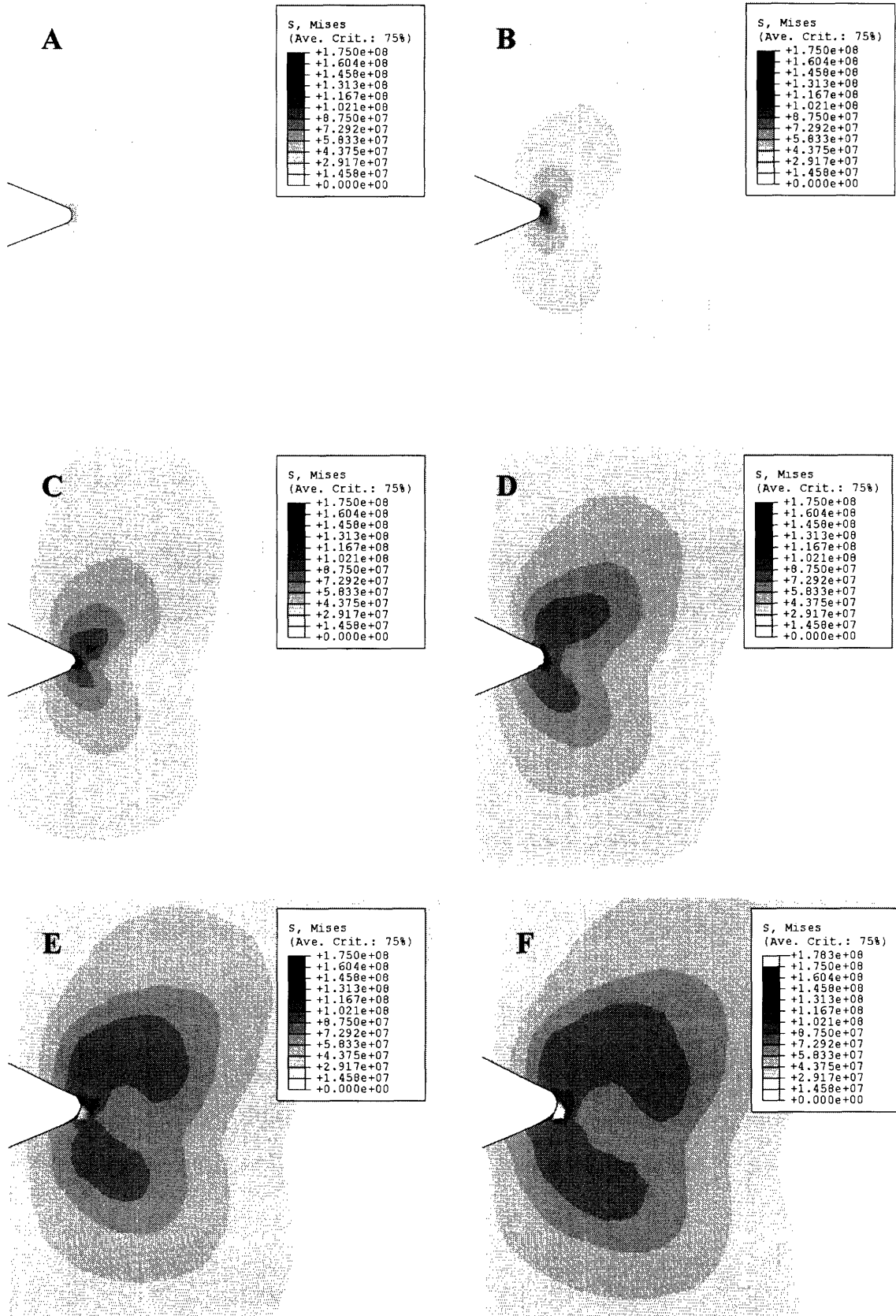
Figure 3.5 Mises stress contours for Izod impact testing of 3.23mm thick specimens.

The corresponding pressure contours for this thin specimen are shown in Figure 3.6 and show that the hydrostatic pressure remains significantly below the Mises stress. Although there is some negative pressure around the notch tip, a large isolated pressure area does not form ahead of the notch. The largest negative pressures seen are observed in areas which have plastically deformed and thus the higher negative pressure regions are simply due to the local strain hardening of the material (i.e they occur after yield, during plastic deformation). This is consistent with the experimental results for the thin specimens for which yield and ductile failure occurs before brittle fracture.
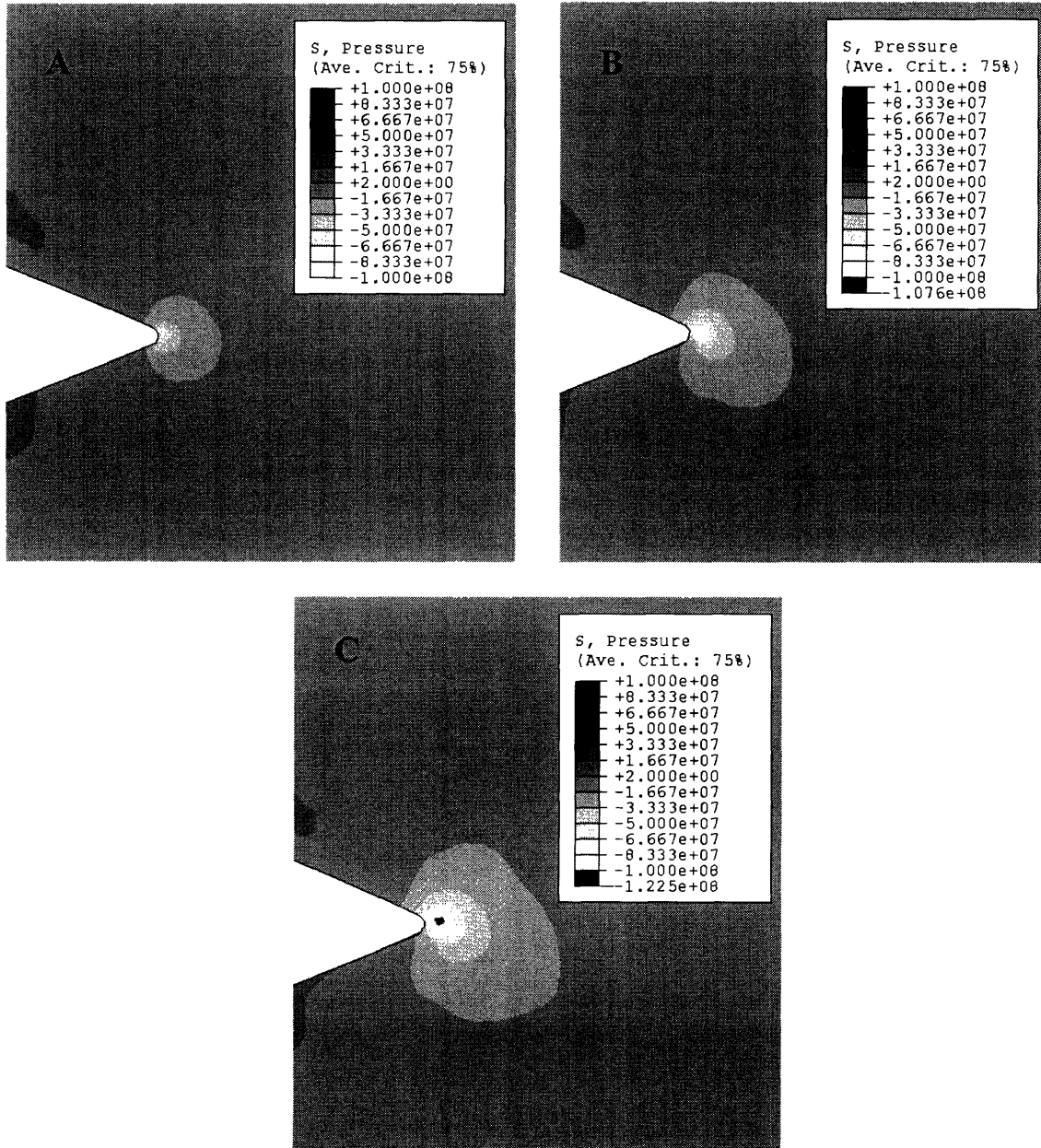

Figure 3.6 Pressure contours for Notched Izod impact testing of 3.23mm thick specimens.

In the early stages of deformation, necking is visible along the outer edge of the notch. Because of the slenderness of the specimen, the outer edge is compliant when the inner portion of the notch begins to stretch. As the pendulum pushes the upper portion of the specimen further, the center of the notch reaches the critical chain stretch at which it begins to tear.
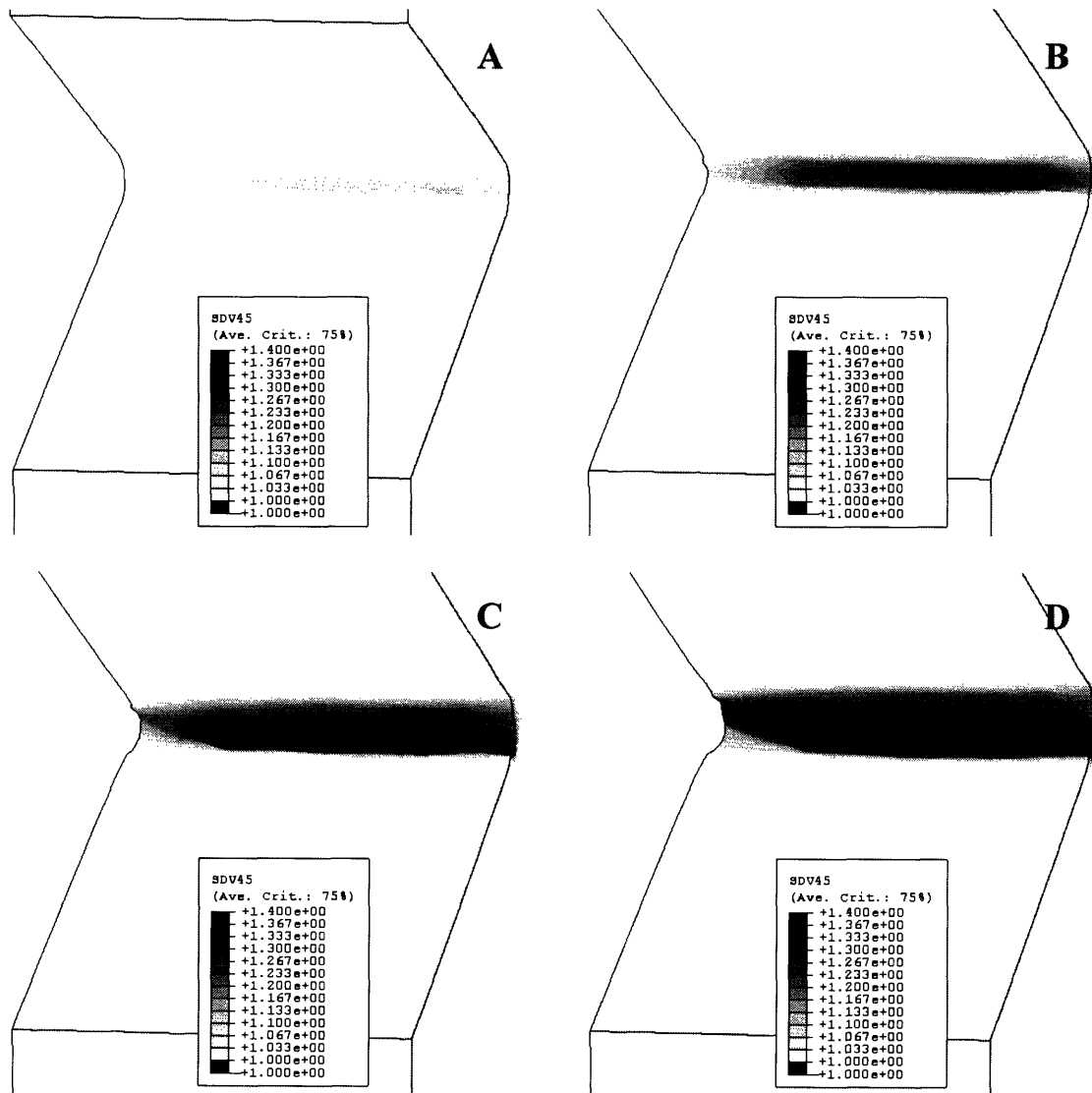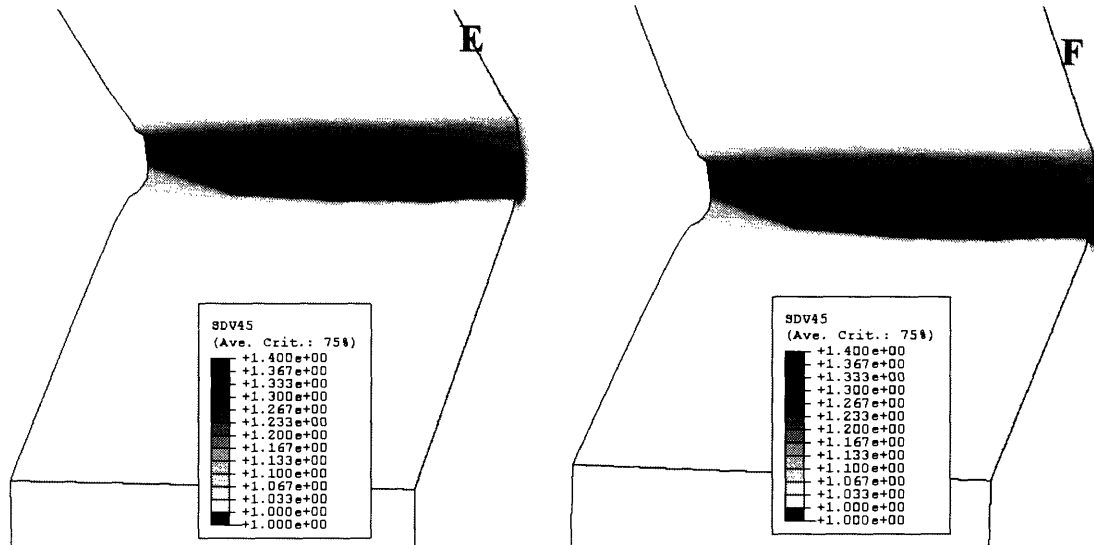
Figure 3.7 Chain stretch at the notch for Notched Izod impact testing of 3.23mm thick specimens(the mid-plane is on the right in all images)

An element begins to become "damaged" at a chain stretch of 1.3. The stress that it carries is reduced relative to the damage value. An element that is designated as fully failed bears no stress (the zero stress elements were apparent on the outer surface in the earlier Mises stress contours). The damage and failure progression of the simulation indicates that at 3.23mm the simulation is nearly plane stress. As shown in Figure 3.8 all but the outer-most elements fail at the same time.**(B)** Just as the outer-most elements fail, the next row deep of elements fail.**(D)** Once tearing has begun at a particular vertical position, it progresses at that level, just as was seen in the experimental results.**(F)**
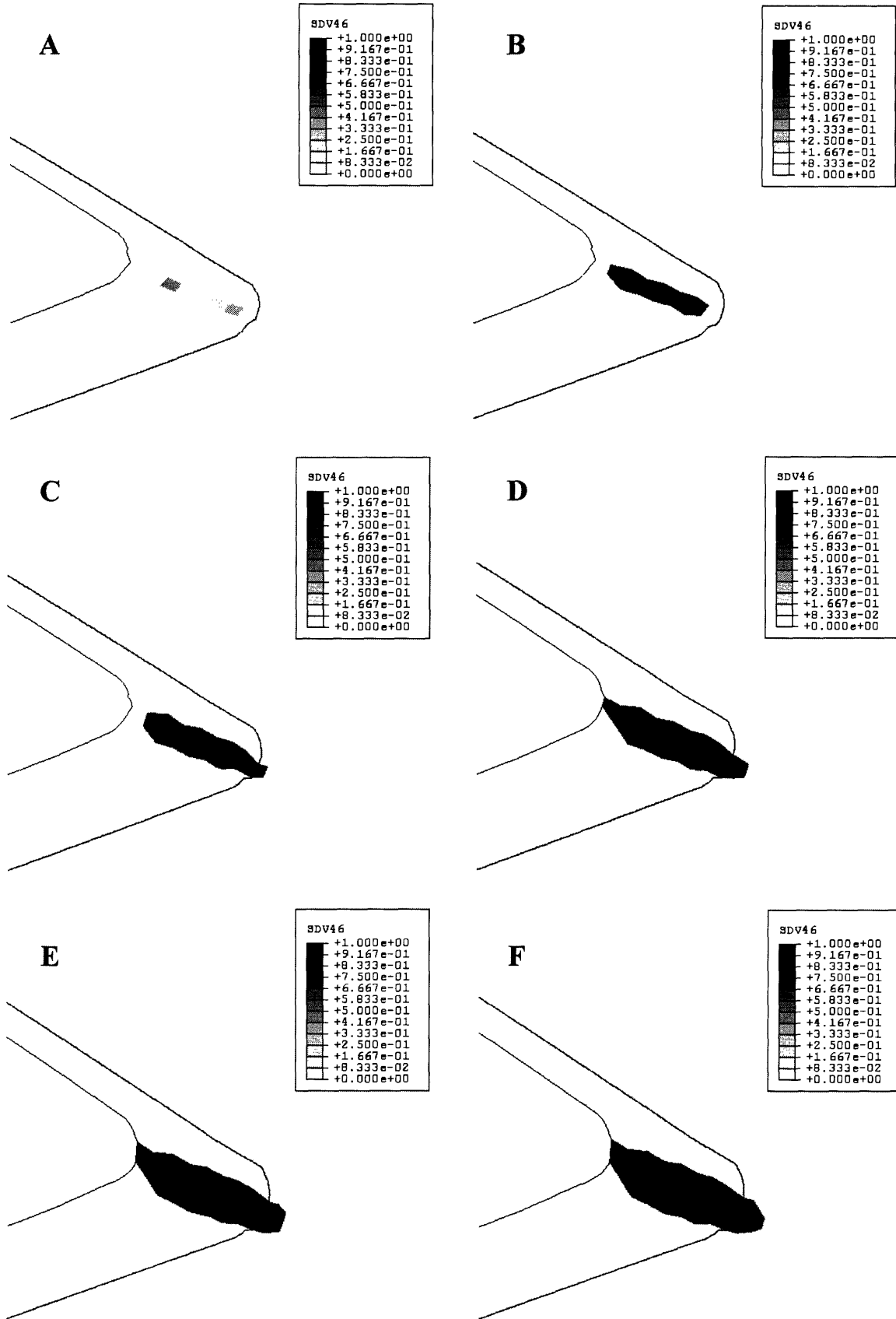
Figure 3.8 Damage in the notch of a 3.23mm thick Notched Izod impact specimen.

Thick (6.35mm thick) Specimen Results:

The results for the model of the 6.35mm thick specimen are shown in Figures 3.9 through 3.13 below. Since the constitutive model does not account for brittle failure, the simulation for the 6.35mm thick specimen was run to the moment at which failure would have initiated. Figure 3.9 shows a wide field view of the Mises stress contours from the time the pendulum hits the specimen to the point where the hydrostatic pressure is great enough that a crack would have formed. Note that as in the thin case, while there is some initial stress at the impact location and stress opposite the notch on the left surface, the stress only becomes large in the notch region.
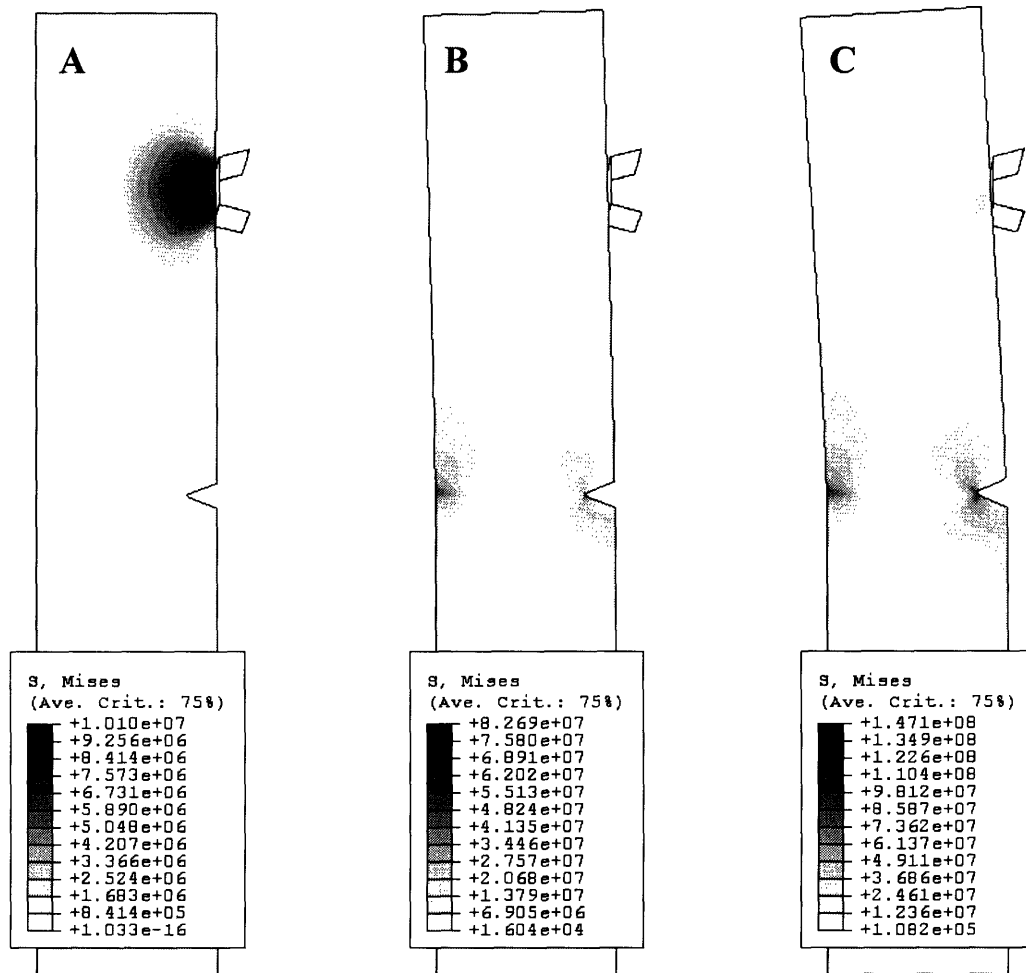

Figure 3.9 Mises stress contours of outer surface impact of 6.35mm thick Notched Izod impact specimen. **A)** at initial impact. **B)** during elastic bending phase **C)** at failure initiation

Figure 3.10 shows the Mises stress around the notch. The stress fields are similarly shaped to those in the 3.23mm model, but they do not grow as large and they do not move away from the front of the specimen since no tearing occurs.
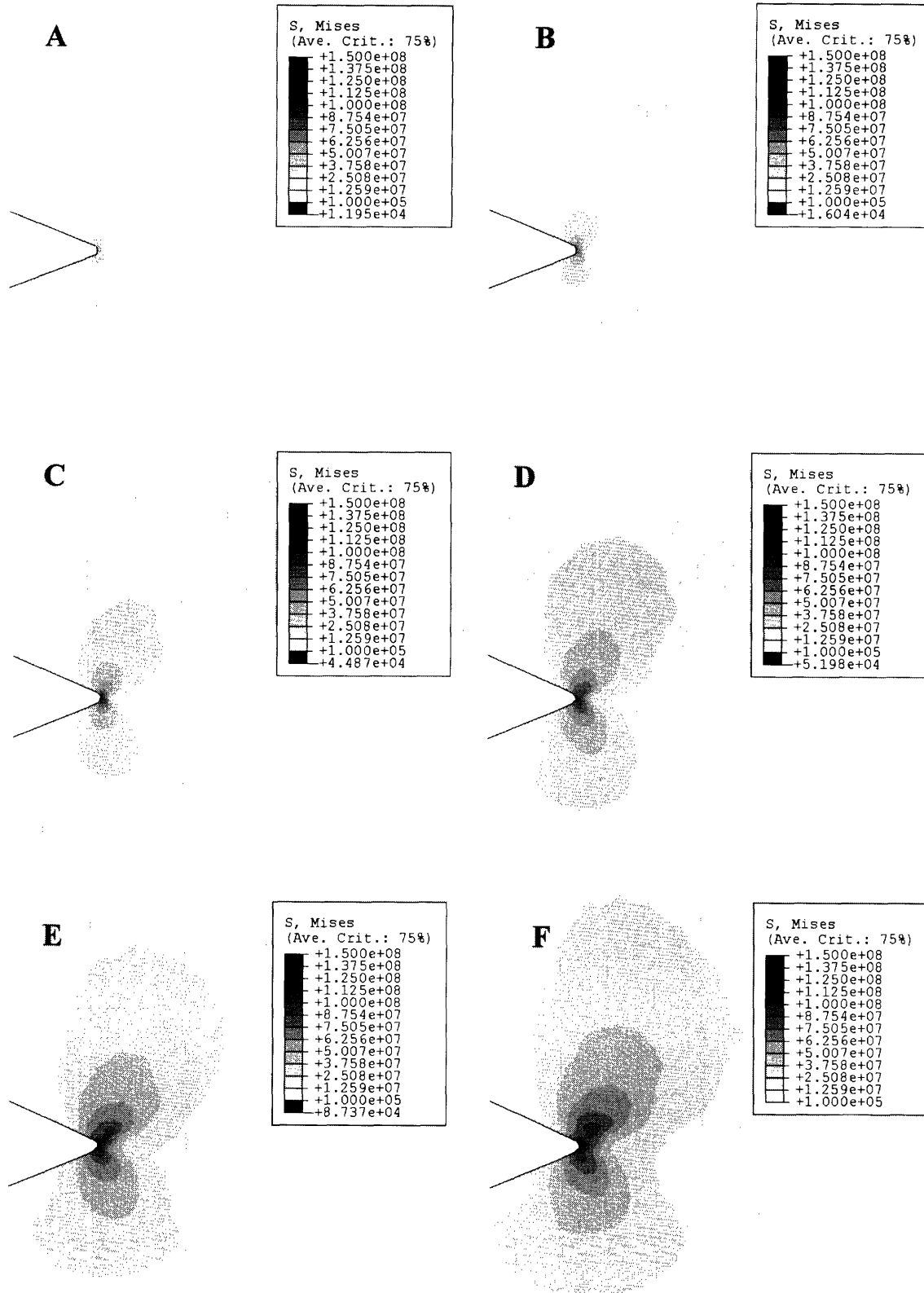
53

Figure 3.10 Mises stress contours on mid-plane for Notched Izod impact testing of 6.35mm thick specimens.

The hydrostatic pressure which causes brittle failure is visible on the inside surface of the specimen, and to a lesser extent on the outside. While there is a strong negative pressure all around the notch, it is centered at a point ahead of the notch rather than at the notch itself. The pressure concentration is not fully developed at this point in the simulation. A finer mesh extending from the notch tip is needed to accurately capture the intersection of the shear band arcs to create the pressure point.
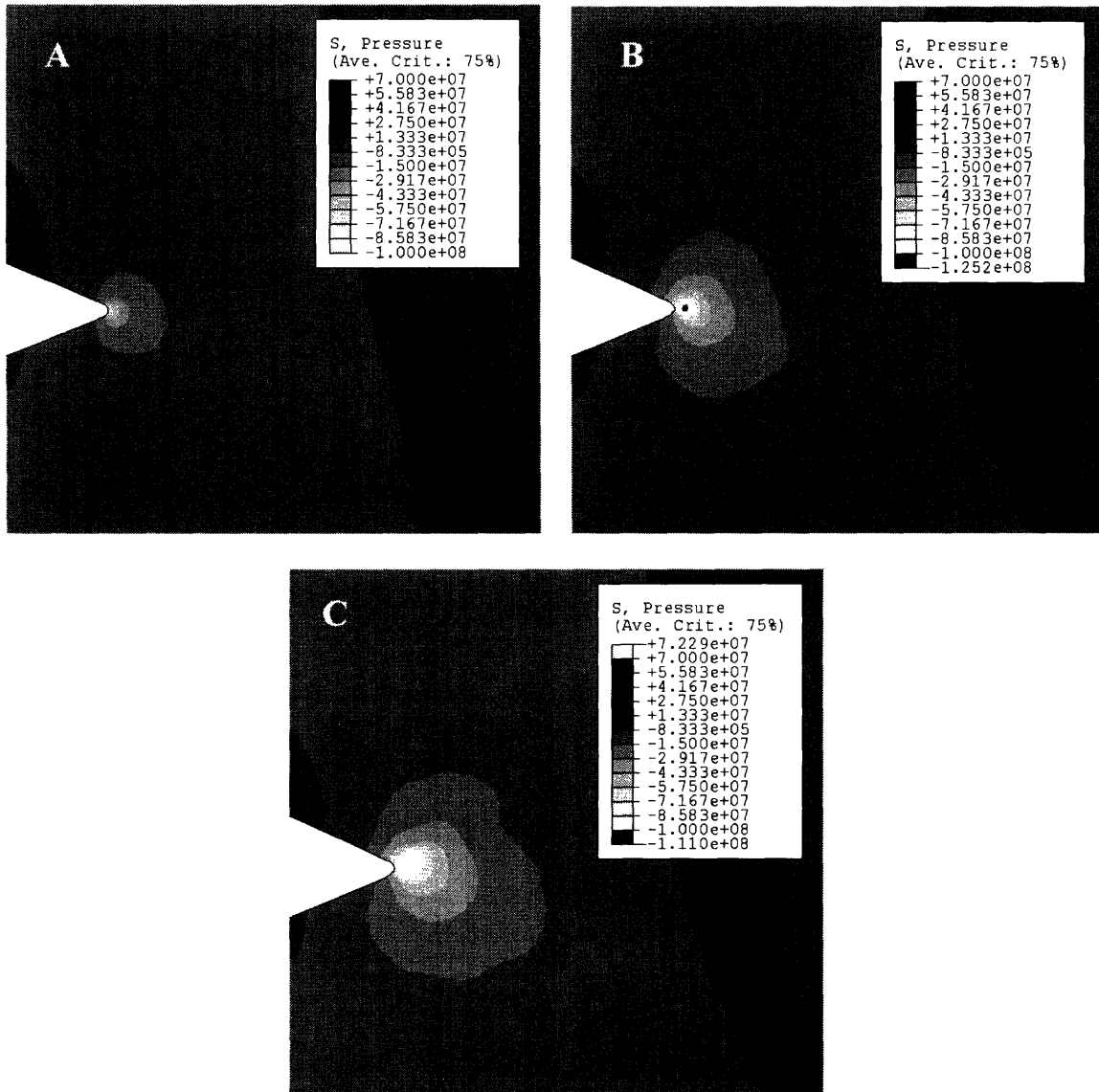
(a)
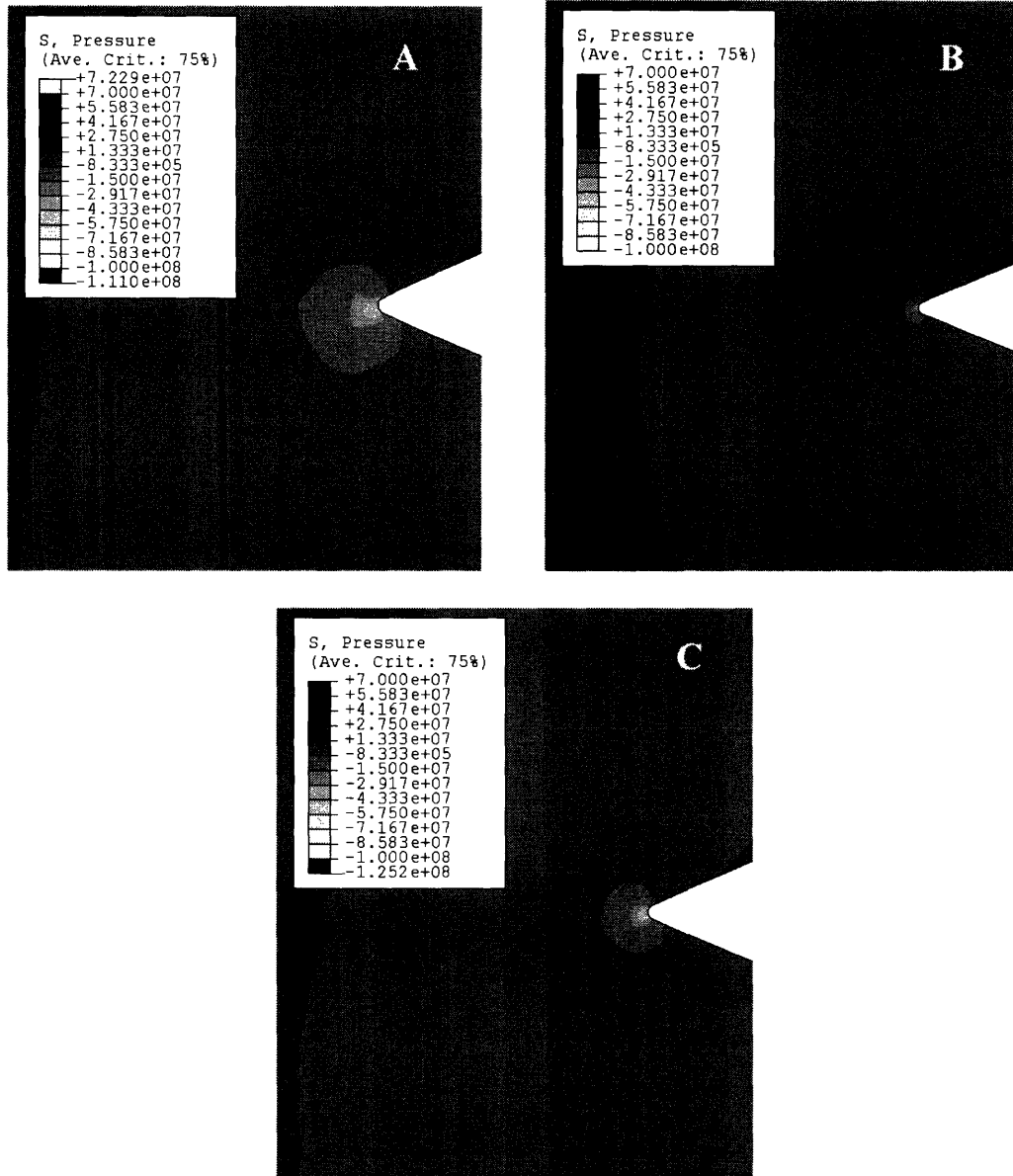
(b)

Figure 3.11 Pressure contours for Notched Izod impact of 6.35mm thick specimens. **a)** mid-plane **b)** outer surface

The model predicts that the crack will initiate 0.2mm from the notch tip. This is a little bit closer to the notch than in the experiment where it initiates 0.9mm from the notch tip. This suggests that we may need to run the simulation slightly longer as well as use a more refined mesh ahead of the notch in future studies.
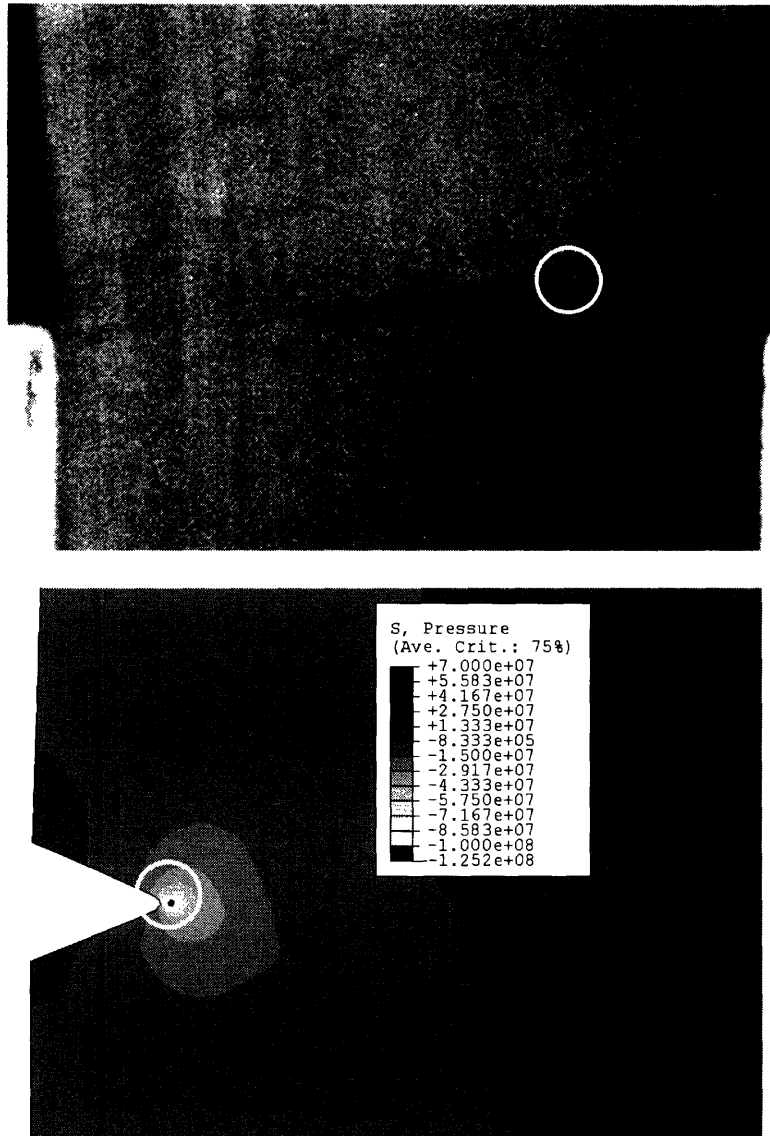
Figure 3.12 Comparison of crack initiation location in experimental and simulation results of Notched Izod impact testing of 6.35mm thick specimen.

The plane strain effects are visible in the lower stress level on the outer edge of the notch. Where on the thin specimen necking was observed, on the thick, it remains undeformed. This is seen in Figure 3.13 which compares the Mises stress and pressure along the notch front of the thick and thin specimens when the pendulum is at the same location.
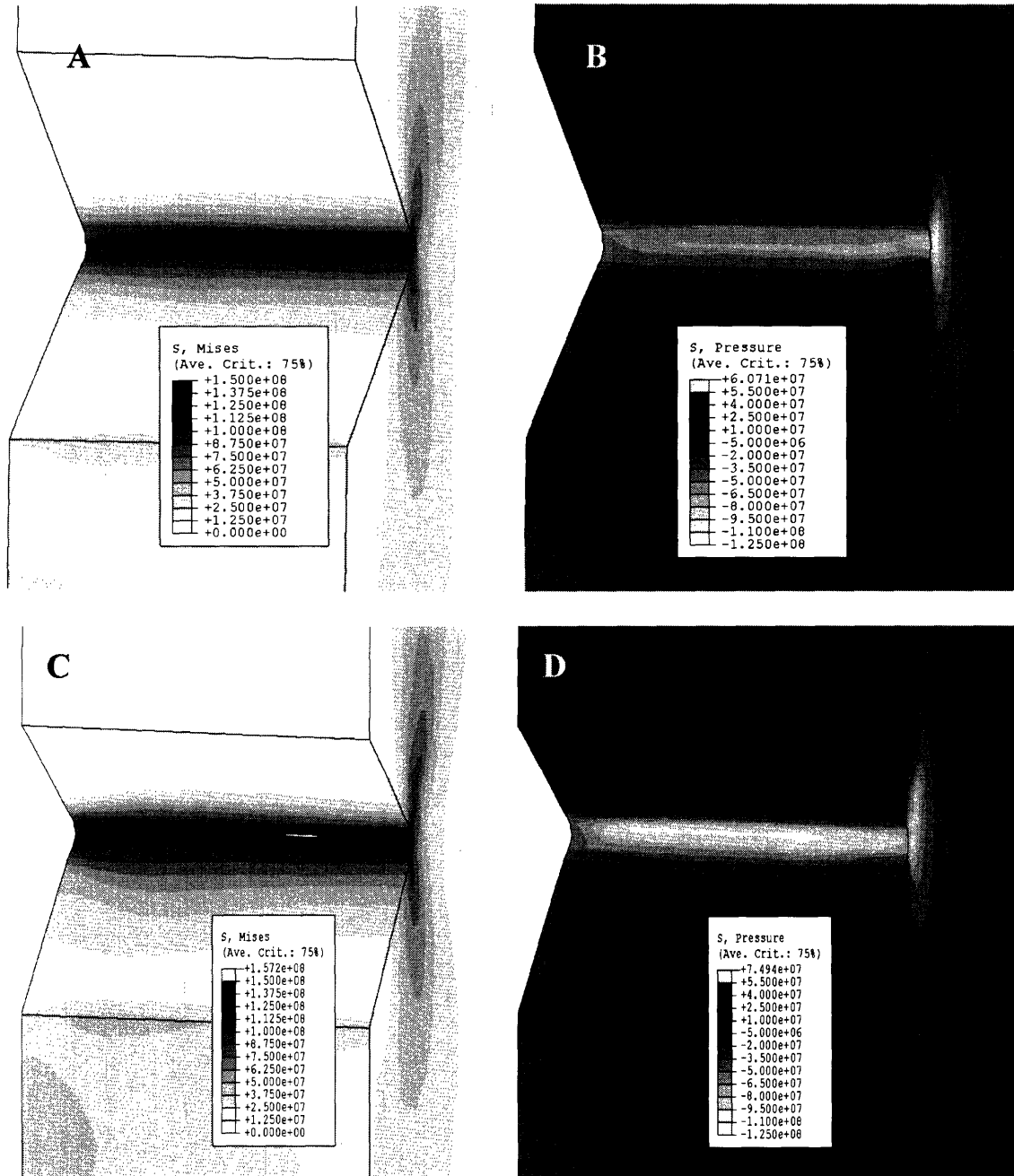
Figure 3.13 Comparison of thick and thin notch Mises stress contours and pressure contours. **A)** Mises stress contour of thin specimen **B)** Pressure contour of thin specimen **C)** Mises stress contour of thick specimen **D)** Pressure contour of thick specimen. (the mid-plane is on the right in all images)

The plane strain condition is also visible from the absence of stress on the outer surface in the direction into the thickness as shown in Figure 3.14.
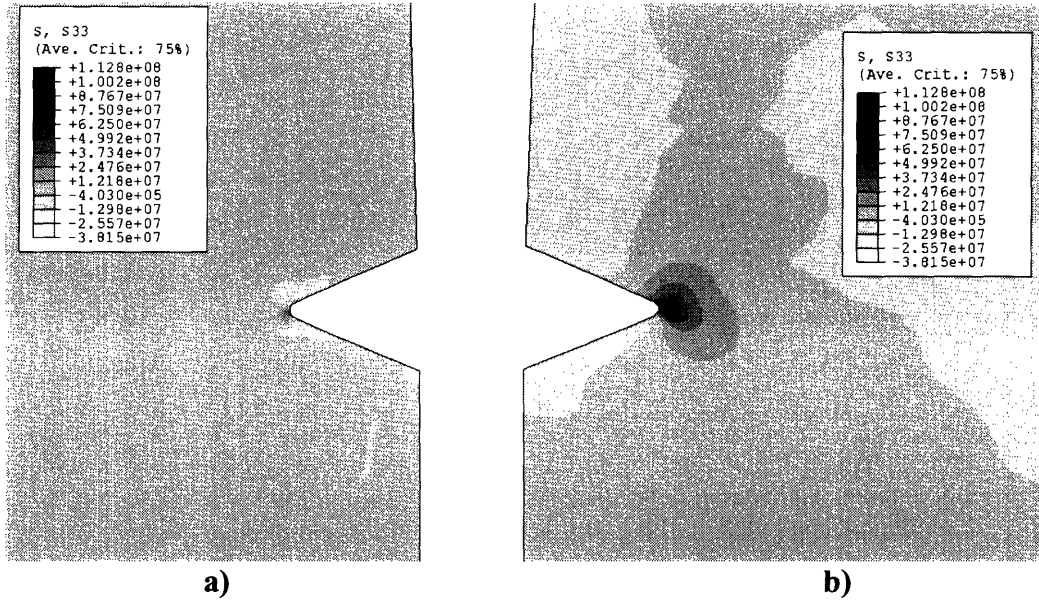
Figure 3.14 Stress in the direction into the thickness for 6.35mm thick specimen on a) outer surface b)mid-plane

In addition to the three-dimensional simulations, a two-dimensional plane strain simulation was conducted for comparison with the 6.35mm thick three-dimensional model. The plane strain pressure concentration (Figure 3.15 B) is greater than the three-dimensional pressure concentration (Figure 3.15 D), while the plane strain Mises stress is smaller.
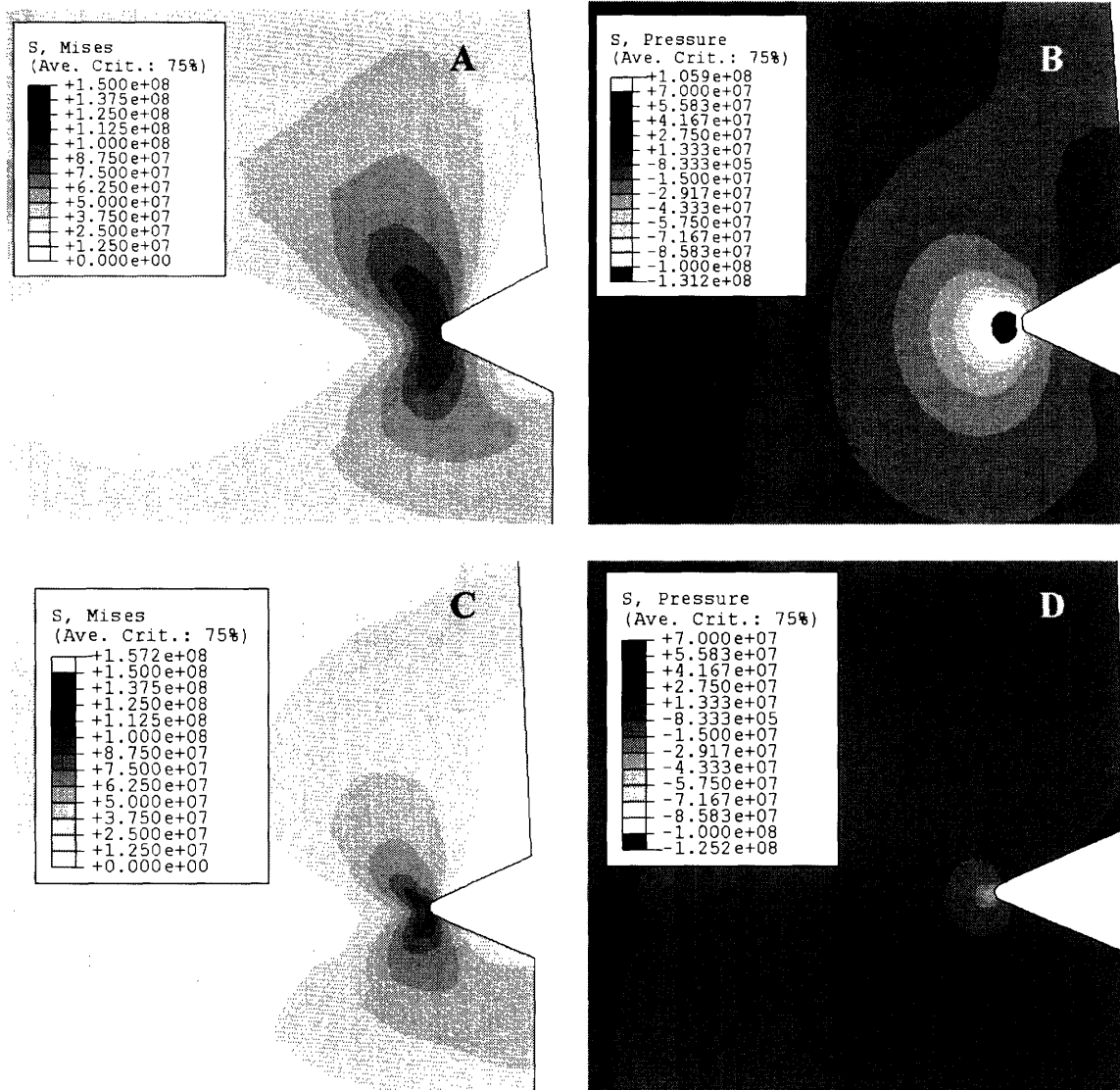
Figure 3.15 Comparison of Mises stress contours and pressure contours of 6.35mm thick two-dimensional plane strain and three-dimension models. **A)** mises stress contour of plane strain **B)** pressure contour of plane strain **C)** mises stress contour of three-dimensional specimen **D)** pressure contour of three-dimensional specimen.

Chapter Four: Conclusions

In this thesis research, Notched Izod impact testing and a Quasi-Static version of the Notched Izod bending mode were conducted on standard Izod specimens of thickness 3.23mm and 6.35mm on the amorphous polymer polycarbonate. The deformation processes were captured by cameras appropriate to the time duration of each test which was dependent on the failure mode and failure progression. In both the Notched Izod impact and the Quasi-Static Izod testing, the 3.23mm specimens underwent a ductile tearing failure and the 6.35mm specimens underwent brittle failure. The 3.23mm specimens deformed elastically followed by extensive yielding at the notch tip; the plastic deformation at the notch tip acted to blunt the notch radius; this was followed by the formation of shear bands extending diagonally across the specimen width from the perimeter of the notch, followed by a tear which then propagated horizontally across most of the width of the specimen leaving a hinged break. Once the tear had initiated, extensive yielding was observed ahead of the propagating tear showing that the failure was preceded by extensive plastic deformation prior to the tearing as the failure propagated across the specimen width. The thick specimens deformed elastically followed by a small amount of local yielding and plastic deformation at the notch tip; the local plastic deformation blunted the notch radius; failure was then observed to initiate ahead of the plastic zone at the notch tip by the formation of a crack ahead of the notch which initiated brittle fracture where the crack propagated back towards the notch as well as across the width of the specimen. The fracture energy per thickness values correlated as expected with the method of failure. The fracture energy per thickness for the thin specimens averaged about seven times greater than that for the thick specimens for both the Notched Izod impact and Quasi-Static Izod tests. The Notched Izod impact fracture energies were 50% higher than the fracture energies for the Quasi-Static Izod tests.

The Arruda and Boyce(1988) constitutive model of polymers as modified by Mulliken and Boyce(2004) for high rate deformation was applied to a three dimensional finite element simulation of the Notched Izod impact test. The 3.23mm thick specimens were modeled from impact through the initiation of tearing. The notch blunting, shear band formation, and tearing that was evident in the experimental images was found in the simulation results as well. The 6.35mm thick specimens were modeled from impact to the formation of a hydrostatic negative pressure point which would cause brittle fracture. The slight yielding and the fracture causing negative pressure in the experimental results were also seen in the model results. Even though the constitutive model has not yet incorporated a brittle failure criterion and therefore is not capable of simulating brittle fracture, the differences in the Notched Izod impact behavior of the thick and thin specimens were illuminated by the simulation results. For the thin specimen the stress was almost evenly distributed across the notch, for the thick specimen the stress was heavily biased towards the mid-plane of the notch; this was one symptom of the difference between nearly plane stress and nearly plane strain which dictated the impact behavior. Future extensions of the constitutive model will incorporate the effects of adiabatic heating. The expressions for the α and β strain rates will also be modified to provide more accurate results for the high strain rates and pressures which are reached during the Notched Izod impact test. Even without these modifications, a model has been

developed which, in conjunction with experimental evidence, provides a qualitative understanding and insight into the failure processes occurring during the Notched Izod impact test which in the past has been used only for quantitative comparisons of the Izod impact energy values for different materials.
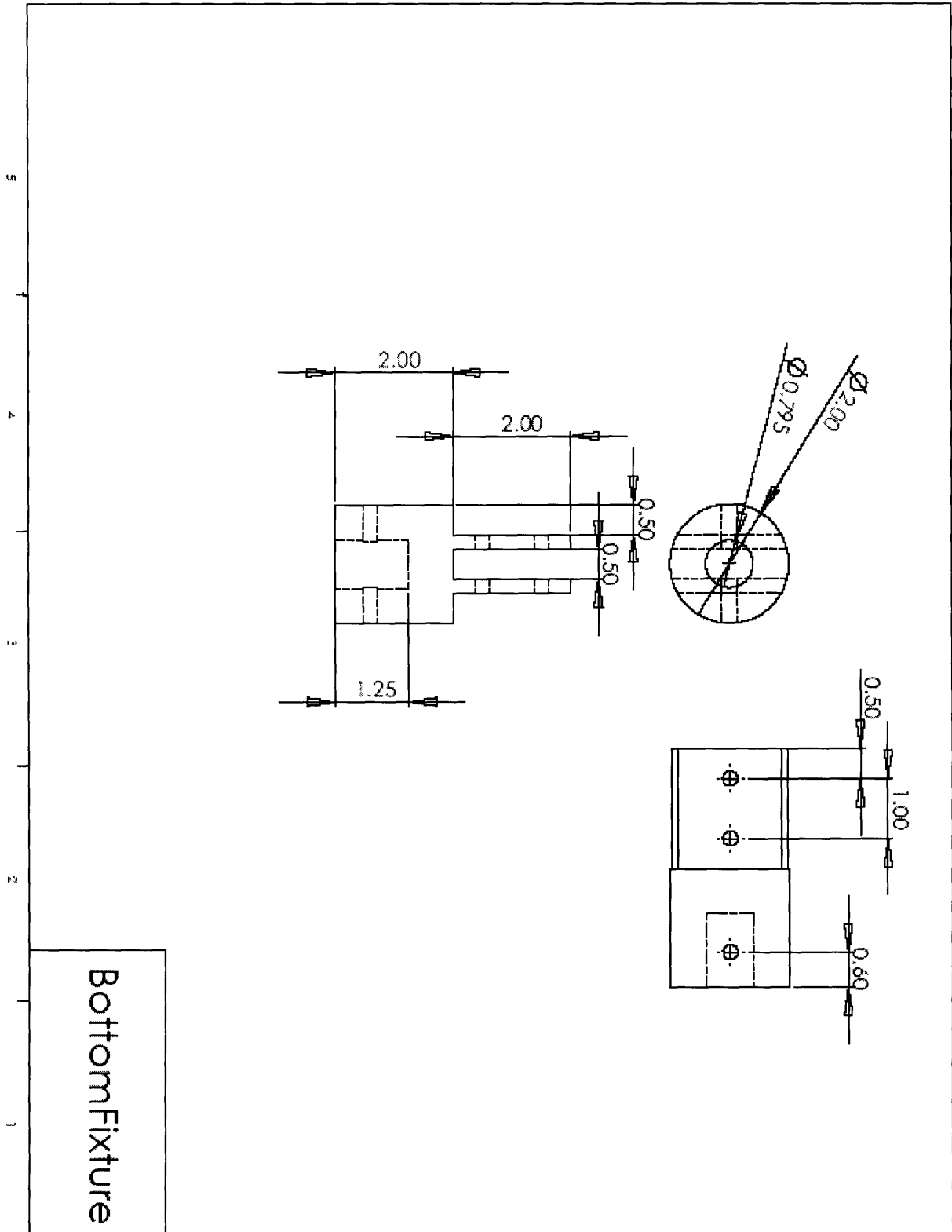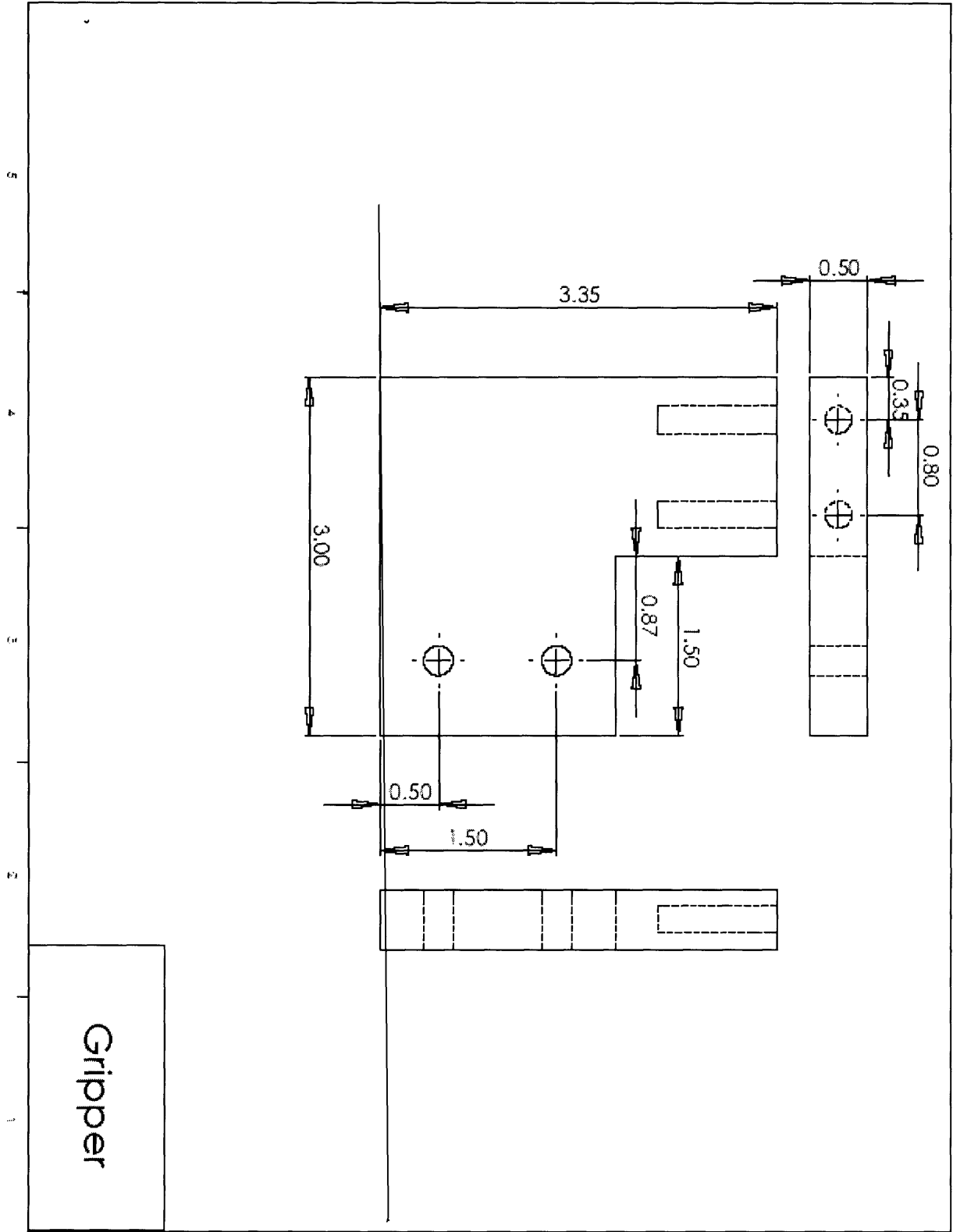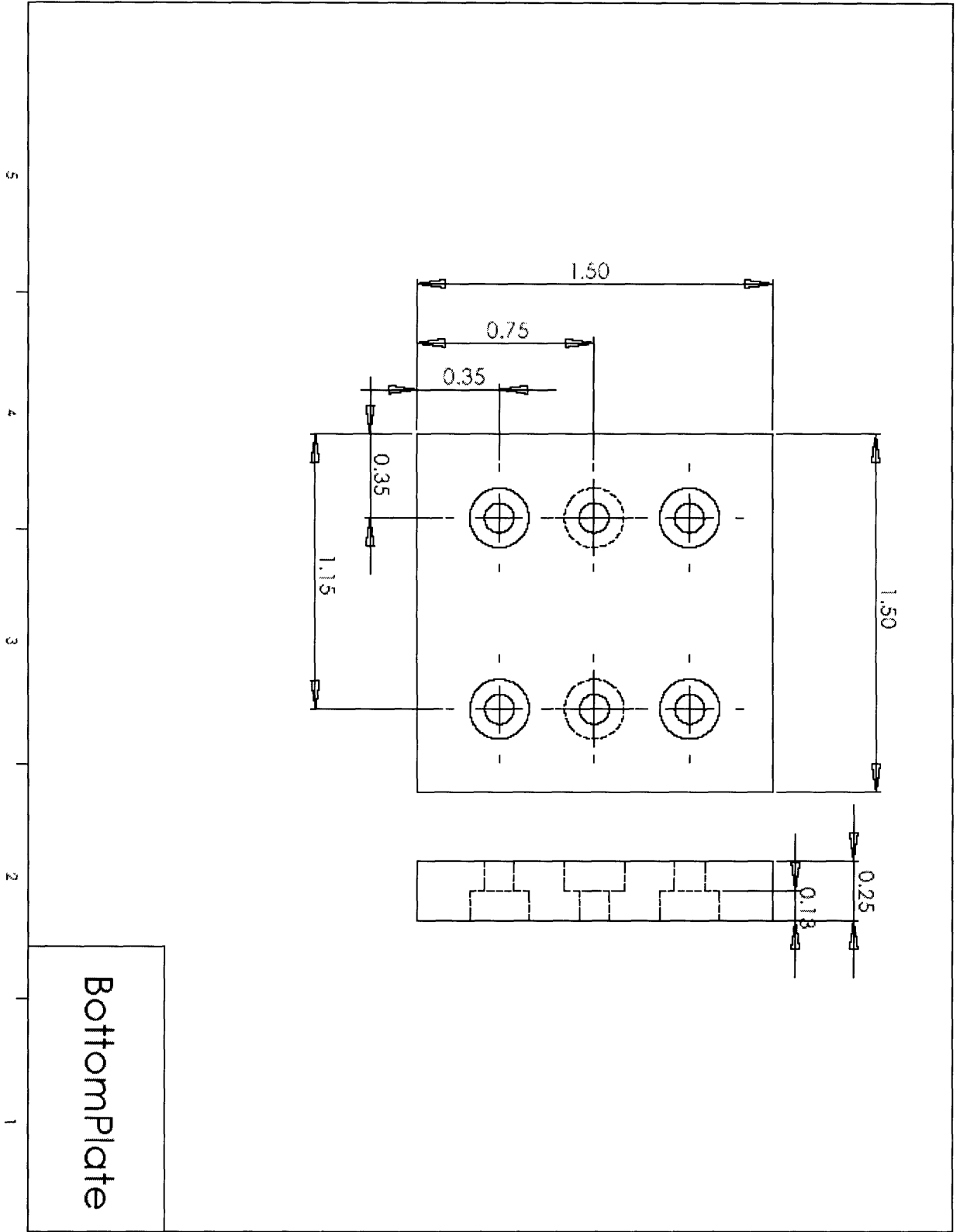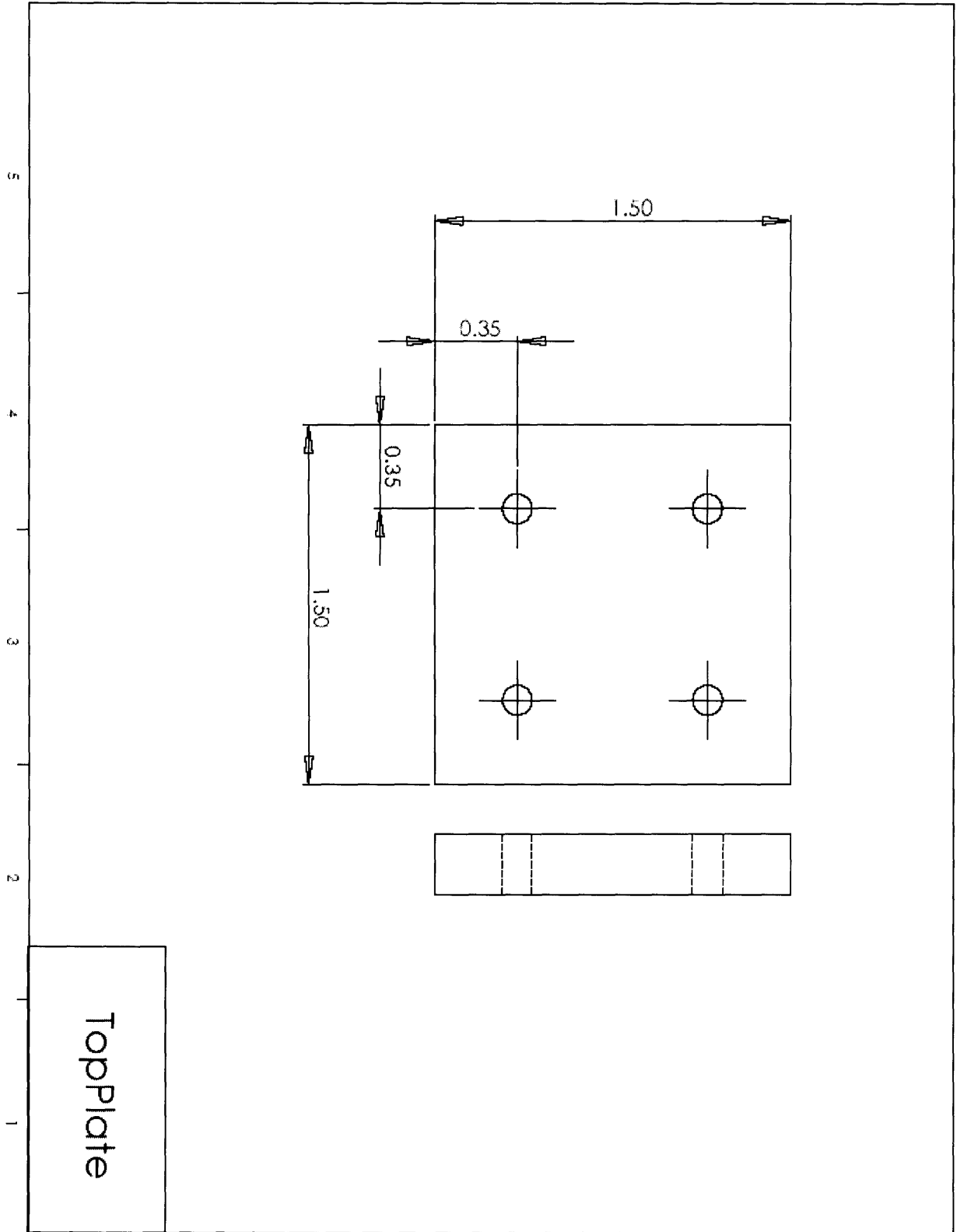
Acknowledgements

References

Standard Test Methods for Determining the Izod Pendulum Impact Resistance of Plastics. ASTM International

Boyce, M., Parks, D., Argon, A., 1988. Large inelastic deformation of glassy polymers. Part I: Rate dependent constitutive model. Mechanics of Materials 7, 15-33

Cheng, C., Hiltner, A., Baer, E., Soskey, P., Mylonakis, S., 1994. Deformation of rubber-toughened polycarbonate: Macroscale analysis of the damage zone. Journal of Applied Polymer Science 177-193

LEXAN® 9034 Sheet. Product Data Sheet. GE Structured Products

Lombardo, B., Keskkula, H., Paul, D., 1994. Influence of ABS type on morphology and mechanical properties of PC/ABS blends. Journal of Applied Polymer Science. 1697-1720

Mulliken, A., Boyce, M., 2005. Mechanics of the rate-dependent elastic-plastic deformation of glassy polymers from low to high strain rates. International Journal of Solids and Structures, in press

Stetz, H., Cassidy, P., Paul, D., 1999. Blends of Bisphenol A Polycarbonate and Rubber-Toughened Styrene-Maleic Anhydride Copolymers. Journal of Applied Polymer Science 1697-1720

Appendix A: Engineering Drawings for Quasi-Static Fixture

2.00

2.00

0.50

0.50

Ø0.795

Ø2.00

1.25

0.50

1.00

0.60

BottomFixture

Gripper

3.35

0.50

0.35

0.80

3.00

0.87

1.50

0.50

1.50

BottomPlate

1.50

0.35

0.35

1.50

TopPlate

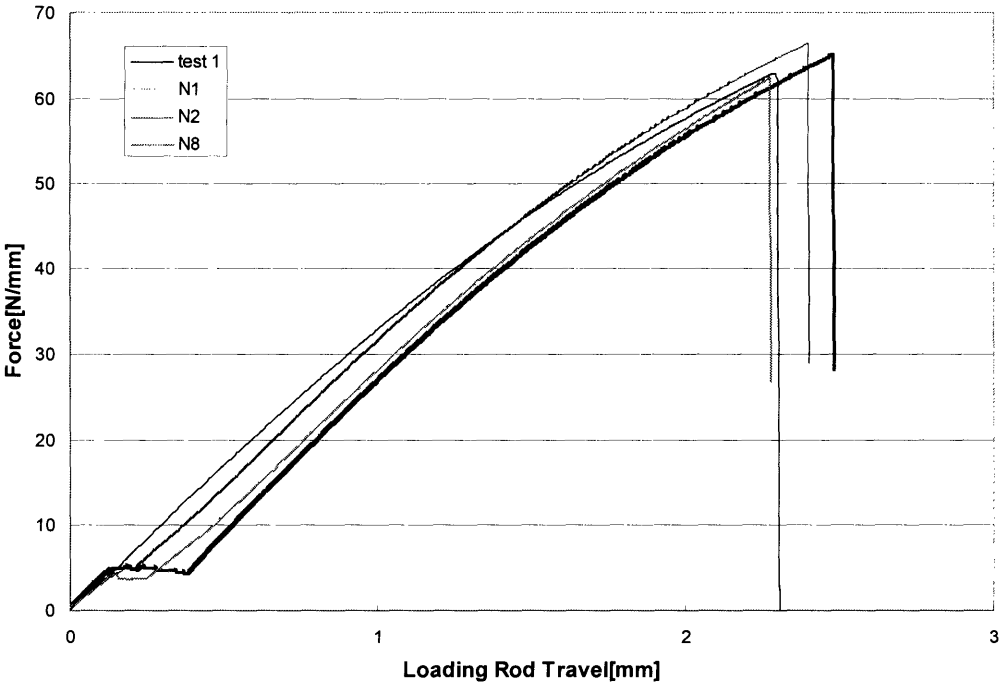# Appendix B: Results for all Quasi-Static Izod tests

Figure B.1 Force-indenter travel curve for specimens of thickness 6.35mm

Figure B.2 Force-indenter travel curve for specimens of thickness 3.23mm